

# Metal Coordination Compounds for Organic Redox Flow Batteries

Jiayi Gao,<sup>[a]</sup> Lixing Xia,<sup>[b]</sup> Miaoning Ou,<sup>[c]</sup> and Zhan'ao Tan<sup>\*[a]</sup>

Along with the continuous optimization of the energy structure, more and more electricity come from intermittent renewable energy sources such as wind and solar energy. Redox flow batteries (RFBs) have the advantage that energy and power can be regulated independently, so they are widely used in large-scale energy storage. Redox active materials are the important components of RFBs, which determine the performance of the battery and the cost of energy storage. Some metal coordination compounds (MCCs) and their derivatives have been considered redox active materials that can replace metal-based redox flow batteries due to their properties such as tunability,

high abundance and sustainability. MCCs can provide higher energy density because they are highly soluble both in the initial state and in any charged state during the battery cycling process. MCCs have also attracted a lot of attention from researchers because of their high economic value, low toxicity, and wide availability. This review provides an overview of the recent development of soluble metal coordination compounds, such as Ferrocene, and concludes with an in-depth discussion of the prospects of metal coordination compounds for application in organic redox flow batteries.

## 1. Introduction

At present, the dominant energy consumption is still fossil fuels such as coal and oil. However, fossil fuels have taken millions of years to form and are non-renewable resources.<sup>[1–5]</sup> The carbon dioxide formed by the combustion of fossil fuels has caused a series of serious environmental problems, such as the greenhouse effect and extreme weather. Therefore, researchers are committed to researching and developing renewable energy sources to meet the current huge energy demand of human society and reduce carbon dioxide emissions.<sup>[6–10]</sup> Renewable energy includes solar energy, wind energy, hydropower, wave and tidal energy, etc. Among them, solar energy and wind energy have been developing rapidly in recent years and have received continuous attention from researchers.<sup>[11,12]</sup> However, photovoltaic power generation and wind power generation have the disadvantages of instability, volatility and randomness, which will cause the grid system to be paralyzed if they are directly integrated into the power grid for power supply.<sup>[13]</sup> In order to improve the utilization of renewable energy and the sustainability of the grid, it is necessary to develop energy storage systems that combine large-scale energy storage devices with renewable energy.<sup>[14]</sup> The new energy storage system represented by electrochemical energy storage has the advantages of fast response speed, flexible project site selection and a short construction period.<sup>[15]</sup> Redox flow batteries (RFBs)

have received widespread attention due to their advantages of long life, good cycling stability, and energy and power that can be designed independently.<sup>[16]</sup> The battery consists of a reaction chamber that can hold two electrodes, a membrane and a flowing electrolyte.<sup>[17]</sup> Most of the current battery electrode materials use carbon felt, and the active materials undergo redox reactions on the surface of the two carbon felts.<sup>[18]</sup> The membrane exists to separate the cathode and anode electrolytes to prevent cross-contamination.<sup>[19–21]</sup> Unlike solid-state batteries, the cathode and anode electrolytes of redox flow batteries are stored independently in two tanks on both sides of the stack and electrolytes are transported to the interior of the battery for reaction through peristaltic pumps and pipelines connected to them, which is capable of providing high energy density.<sup>[22]</sup> The energy of the battery is closely related to the volume and concentration of the cathode and anode materials.<sup>[23]</sup> Redox flow batteries have special structures. As long as there are enough electrolytes in the tanks, the energy of the battery is theoretically unlimited.<sup>[24]</sup> The power of the RFBs depends on the number of battery stacks and the area of the electrode material. In this regard, the energy and power of the RFBs can be freely adjusted according to the needs.<sup>[25–28]</sup> RFBs are safer and less likely to explode or have other safety incidents. The RFBs have a long cycle life, and the redox active materials can be recycled and reused many times to support deep charge and discharge.<sup>[29–32]</sup> The basic configuration of the RFBs is shown in Figure 1 below. The characteristics of some active species in organic redox flow batteries and the cycling performance of some organic redox flow batteries systems are given in Tables 1 and 2, respectively.

Since Thaller proposed the concept of RFBs in 1974,<sup>[33]</sup> significant progresses have been made in this field.<sup>[34–37]</sup> Currently, vanadium and zinc-based RFBs are relatively mature systems. Although these battery systems have entered the stage of demonstration applications, there are still many

[a] J. Gao, Z.a. Tan  
Beijing Advanced Innovation Center for Soft Matter Science and Engineering, Beijing University of Chemical Technology, Beijing 100029, China  
E-mail: tanzhanao@mail.buct.edu.cn

[b] L. Xia  
China Electric Power Research Institute, Beijing 10000, China

[c] M. Ou  
School of Materials Science and Engineering, Beijing University of Chemical Technology, Beijing 100029, China

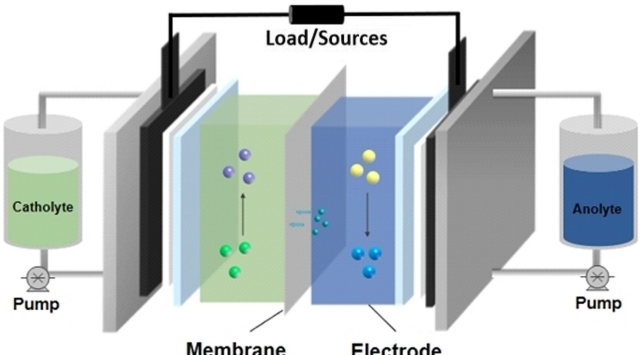


Figure 1. Schematic diagram of redox flow battery structure.

challenges.<sup>[38]</sup> For example, zinc-based RFBs typically have the shortcomings of limited surface capacity, zinc dendrites, and low operating current density, while VRFBs are characterized by the high cost of ion exchange membranes and electrolytes.<sup>[39–41]</sup> Until now, most RFBs still use inorganic redox materials as cathode and anode active materials, and the redox reaction of such materials is mainly dependent on the valence change of the metal center, and in some designs, precious metals may be required as catalysts to accelerate the electrochemical reaction process.<sup>[42]</sup> The electrochemical activity of metal-based RFBs is constrained by the inherent properties of inorganic redox materials, and the difficulties in further increasing the energy density limit their further development and application.<sup>[43]</sup> In order to solve the challenges posed by metal-based redox active materials, the search for green and inexpensive active materials for RFBs is imminent.

In recent years, through the continuous exploration of researchers, organic redox molecules have become a promising redox active material that can be applied to RFBs.<sup>[44]</sup> Organic redox molecules can be synthesized or directly obtained from sustainable and renewable natural resources, with the advantages of low cost, scalability, efficient biodegradation and low environmental impact. MCCs can be stabilized in a variety of oxidation states, and most of them have high solubility in organic solvents, which are good active materials for ORFBs.<sup>[45–48]</sup> In addition, structures and properties of metal ions or ligands can be customized through molecular engineering, such as grafting different functional groups on organic molecules to obtain MCCs with high stability, good solubility

and large redox electric pair potential difference. In this paper, the latest research progress of MCCs in ORFBs in recent years is reviewed.<sup>[49]</sup>

## 2. Redox Flow Batteries (RFBs)

The concept of RFBs was originally proposed by Thaller in 1974. It is a new kind of medium- and large-scale electrochemical energy storage device that is suitable for use in combination with renewable energy sources and easy to use for large-scale power storage.<sup>[33]</sup>

### 2.1. Basic Principles

The performance evaluation parameters of RFBs are mainly discharge capacity (DC), coulombic efficiency (CE), voltage efficiency (VE), and energy efficiency (EE), which can be obtained from battery charging and discharging platforms, such as LANHE.<sup>[50]</sup> The DC refers to the value of the capacity that the battery can output under certain test conditions, and the larger value indicates that the battery is more capable of storing electricity under these conditions.<sup>[51]</sup> CE is the ratio of DC to charge capacity. The longer the charge/discharge time, the greater the charge loss the lower the CE will be. VE is commonly used to characterize the degree of polarization during battery charging and discharging. It can reduce the degree of polarization during battery charging and discharging by accelerating charge transfer and ion diffusion, effectively improving battery performance. EE is the product of VE and CE.<sup>[52]</sup>

### 2.2. Types of Organic Redox Flow Batteries (ORFBs)

Organic redox flow batteries (ORFBs) replace the metals and halogens used in conventional RFBs with organic redox active materials.<sup>[53]</sup> The electrochemical reactions of ORFBs are similar to that of VRFBs, which occur without additional catalysts and do not generate dendrites during the charging and discharging process.<sup>[54]</sup> Most of the constituent elements of organic redox active materials are C, H, O, N, etc., and such elements are abundant and widely available. In addition, organic redox active



Zhan'ao Tan is a professor in Beijing Advanced Innovation Center for Soft Matter Science and Engineering, Beijing University of Chemical Technology. He received his Ph.D. degree in physical chemistry in 2007 from Institute of Chemistry, Chinese Academy of Sciences and then came to Pennsylvania State University, USA, as a postdoctoral from 2007 to 2009. His present research interests include polymer solar cells, semiconductor nanocrystal-based optoelectronics, organic-inorganic hybrid perovskite solar cells, and flow batteries.



Jiayi Gao received her bachelor's degree in energy chemistry and engineering from North China University of Science and Technology in 2023. She is currently pursuing her master's degree under the supervision of Prof. Zhan'ao Tan at Beijing Advanced Innovation Center for Soft Matter Science and Engineering at Beijing University of Chemical Technology. Her research interests mainly focus on organic redox flow batteries.

**Table 1.** Characteristics of some active species in organic redox flow batteries.

Active species	Solvent	Solubility	Scan rate	Redox potential	Reference
Fc-SO <sub>3</sub> Na	H <sub>2</sub> O	2.5 M	100 mVs <sup>-1</sup>	E <sub>1/2</sub> = 0.13 V vs. Ag/AgCl (Na <sub>2</sub> SO <sub>4</sub> )	[76]
Fc-SO <sub>3</sub> NH <sub>4</sub>	H <sub>2</sub> O	0.41 M	100 mVs <sup>-1</sup>	E <sub>1/2</sub> = 0.38 V vs. Ag/AgCl (NH <sub>4</sub> Cl)	[77]
P2 + BTMAPV	C <sub>6</sub> H <sub>5</sub> Cl	1.0 M	5 mVs <sup>-1</sup>	1 V vs. Ag/AgCl (NaCl)	[84]
Fc4Ph-TFSI	DMF	2.27	100 mVs <sup>-1</sup>	1.96~2.06 V vs. Ag/AgCl (TEATFSI/DMF)	[86]
Fc1 N112-Br	H <sub>2</sub> O	2.9	10 mVs <sup>-1</sup>	0.43 V vs. Ag/AgCl (H <sub>2</sub> O)	[90]
Fc3/Fc4	H <sub>2</sub> O	0.66 M/2.01 M	10 mVs <sup>-1</sup>	E <sub>1/2</sub> = 0.456, 0.453 V vs. Ag/AgCl (NaNO <sub>3</sub> )	[95]
Cr(L3) <sub>3</sub>	H <sub>2</sub> O	1 M	100 mVs <sup>-1</sup>	E <sub>1/2</sub> = -0.18 V (1 <sup>st</sup> ) vs. Ag/AgCl (TBA)BF <sub>4</sub>	[101]
Fe <sup>III</sup> (acac) <sub>3</sub>	MeCN	> 1 M	50~2500 mV	E <sub>1/2</sub> = -0.61 V vs. Ag/AgCl (TBAPF <sub>6</sub> )	[110]

#: Data is estimated basing on graphic coordinates

**Table 2.** Cycling performance of some organic redox flow batteries systems.

Active species	Electrolyte	membrane	Cycle number	Current density	Coulombic efficiency	Energy efficiency	Discharge capacity retention ratio
Fc-SO <sub>3</sub> Na/Zn	Na <sub>2</sub> SO <sub>4</sub>	(SPEEK/TiO <sub>2</sub> ) composite membrane	1000	80 mA cm <sup>-2</sup>	100%	–	97.8%
BASFc/V <sup>3+</sup>	H <sub>2</sub> SO <sub>4</sub>	Nafion 212	120	60 mA cm <sup>-2</sup>	100%	> 70%	87.64%
Fc/FcB4F <sub>4</sub>	TEA BF <sub>4</sub>	High porosity glass frit	200	2.4 mA cm <sup>-2</sup>	–	–	80%
p(FEMA-co-SBMA)/BTMAPV	NaCl	FAA-3~50 anion exchange membrane	100	–	> 99%	–	–
Fc4Ph-TFSI/ Fc4Ph-TFSI	1,3-dioxo-lane	Daramic-250	50	20 mA cm <sup>-2</sup>	94.6%	77.7%	99.8%
Fc1 N112-Br/Zn	HCl	SF600	20	5 mA cm <sup>-2</sup>	95.7%	–	> 99%
FcNCl/MV	NaCl	Selemon AMV	700	60 mA cm <sup>-2</sup>	99%	60%	~99.8%
[Co(bpy) <sub>3</sub> ] <sup>2+</sup> /Li	EC-DM	Li-ion-conductive glass ceramic separator	20	0.5 mA cm <sup>-2</sup>	99.9%	73%	99.1%
Fe(acac) <sub>3</sub> /Cr-(acac) <sub>3</sub>	TEA BF	NafionSi	50	5 mA cm <sup>-2</sup>	99%	53%	–

#: Data is estimated basing on graphic coordinates.

materials can be used to realize a green battery cycle in a low-carbon emission way, as shown in Figure 2 below.<sup>[6,55]</sup> ORFBs are categorized into two types according to the redox active materials or solvents. One is aqueous organic flow batteries (AORFBs), and the AORFBs can be classified into acidic, alkaline and neutral systems according to the pH of the electrolyte, the other type is non-aqueous organic flow batteries (NAORFBs). The scope of ORFBs discussed in this paper is that, in water or organic solvents, one side of the cathode and one side of the anode can be used with an organic molecule as the solute.<sup>[56]</sup>

### 2.3. Aqueous and Non-Aqueous Organic Redox Flow Batteries

Aqueous redox flow batteries (ARFBs) use water as a solvent for the electrolyte, and when the electrolyte of the ARFBs is organic compounds, the batteries are called aqueous organic redox flow batteries (AORFBs).<sup>[57]</sup> By using water as the solvent, AORFBs can get a higher rate of electrochemical reactions and faster conductivity of the electrolyte.<sup>[58]</sup> However, the narrow electrochemical window of water (1.23 V) limits the energy

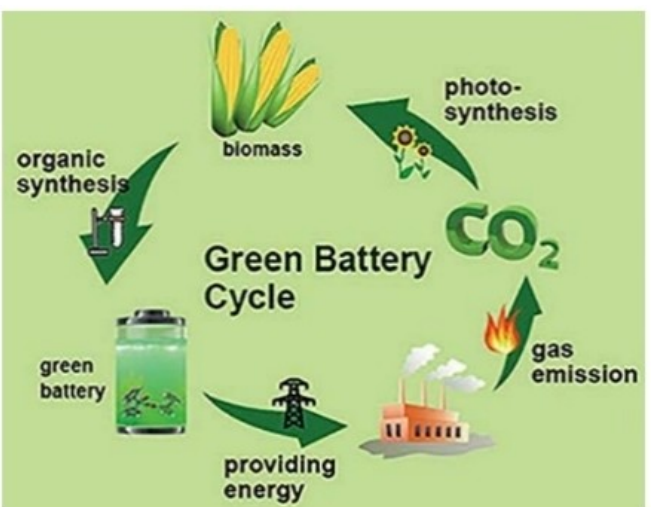


Figure 2. Ideal green battery cycle with a low carbon footprint. Adapted with permission from Ref. [6] Copyright (2017) Wiley-VCH Verlag GmbH & Co. KGaA, Weinheim. All rights reserved.

density of AORFBs. This problem is solved by attaching hydrophilic groups, such as hydroxyl ( $-OH$ ), sulphonic acid ( $-SO_3H$ ) and quaternary ammonium ( $-N^+(CH_3)_3$ ) groups, to organic molecules that are otherwise insoluble or poorly soluble in water, in order to increase the solubility of organic redox active materials in water. The connection of these groups also helps to change the half-wave potential of the organic active materials and increase the voltage to improve the energy density of the batteries.<sup>[59]</sup> With continuous attempts by researchers, it has been found that organic solvents have wide electrochemical windows to increase the energy density of RFBs effectively, and such RFBs using organic solvents are called non-aqueous redox flow batteries (NAORFBs). Commonly used organic solvents are dimethoxyethane (DME), acetonitrile (MeCN), ethylene carbonate (EC), etc.<sup>[60]</sup> These solvents have wide electrochemical windows, and higher voltages can also be obtained. Compared to AORFBs, the choices of solvents and electrolytes for NAORFBs are more flexible. In addition, whether it is AORFBs or NORFBs, the stabilities of the redox active materials during the charging and discharging process will affect the DC of the batteries, so NORFBs have greater advantages than AORFBs in the selection of redox active materials and solvents.<sup>[61]</sup>

### 3. Classification of Metal Coordination Compounds

MCCs not only have high solubility in the initial redox state but also have high solubility in all charged states after the battery enters the subsequent cycle process. High solubility helps improve the charge and discharge capacity (DC) of the batteries and improves battery performance.<sup>[62]</sup> In this paper, MCCs are roughly divided into two categories: organic metal coordination compounds and inorganic metal coordination compounds, and MCCs that have been used in organic redox flow batteries are discussed. The complexes formed by ligands and metal atoms or metal ions through coordination bonds are called MCCs. Organic metal coordination compounds (OMCs) consist of organic parts and metal active groups, and by skillfully designing different molecular structures or combining functional groups with different functions, a variety of active materials can be created to meet the requirements. Inorganic metal complexes, on the other hand, are composed of inorganic parts and metal active groups.<sup>[63]</sup>

The organic metal coordination compounds that have been applied in energy storage batteries are MOFs, porphyrin compounds, phthalocyanine Ferrocene etc.<sup>[64–69]</sup> The metal ions in MOF are able to undergo multiple valence changes in the redox reaction process, so they have a high charging and discharging capacity. The porphyrin complexes are formed by the bonding of the central metal ion with the four nitrogen atoms in the heterocyclic ring. The reason for their redox activity is that, in the porphyrin coordination compounds, the metal ion is the electron acceptor, and the nitrogen atoms are the electron donors. Ferrocene shows excellent electrochemical performance in RFBs, and during the reaction, the iron ion is

able to carry out reversible redox. The phthalocyanine (Pc) complex consists of a central transition metal ion and a large, conjugated ligand in which the nitrogen atoms can provide additional electrons, thus promoting the catalytic performance of the metal ion.

In addition to the above common MCCs, new organic materials that can be used in RFBs have also been proposed by researchers, such as fullerene derivatives that have the ability to accept multiple electrons and undergo very fast and stable redox processes based on fullerene cages. Utilizing multiple metallocene moieties appended to the fullerene cage as the catholyte species, while exploiting the inherent, reversible redox processes of the fullerene moiety as the anode-active species to assemble the battery system, this system demonstrates a new concept in redox electrochemistry of RFBs. With further work, fullerene-based batteries have the potential to achieve even further development by increasing current and energy density.<sup>[70]</sup>

## 4. Various Functional Ferrocene is Used in Organic Redox Flow Batteries

### 4.1. Sulfonate Function of Ferrocene

At present, there have been studies using amethyst derivatives as active materials for organic redox flow batteries. Because the performance of ORFBs depends on the concentration of the electrolyte, the battery performance can be improved only at high concentrations. However, a high concentration of amethyst derivatives is very dangerous.<sup>[71–73]</sup> Functional ferrocene derivatives are one of the most promising electroactive organic electrolytes. The bottleneck problems of their application in water redox flow batteries are poor solubility, low potential and complexity of modification methods to solve these problems.<sup>[74]</sup> Functional Ferrocene with good solubility and excellent reversible redox activity can be obtained by designing ferrocene molecules through molecular engineering.<sup>[75]</sup> The current selection of viable cathode electrolytes is still limited, which is further limited by the incompatibility of positively charged redox materials with cation exchange membranes. YU et al.<sup>[76]</sup> reported an anionic sulfonated ferrocene derivative with a negatively charged part to solve the above problem. The anion  $Fc-SO_3^-$  was obtained by grafting bis(propyl-sulfonate) group onto the Cp rings of insoluble Ferrocene (Figure 3a). Due to the modification of sulfonic acid group, the solubility of  $Fc-SO_3Na$  in water was greatly improved (2.5 M). They assembled a flow battery with  $Fc-SO_3Na$  as the cathode active substance and zinc metal as the anode (Figure 3b). The test results show that the battery has excellent capacity retention performance, with no significant capacity attenuation within 800 cycles and a capacity retention rate of 97.5% after 1000 cycles. It is noteworthy that the CE of the battery remained nearly consistent throughout the cycle test (Figure 3c). The cathode solution has a volumetric capacity of  $67.0\text{ Ah L}^{-1}$ . At low concentrations, the battery's capacity retention rate is 99.9975%, and at high concentrations,

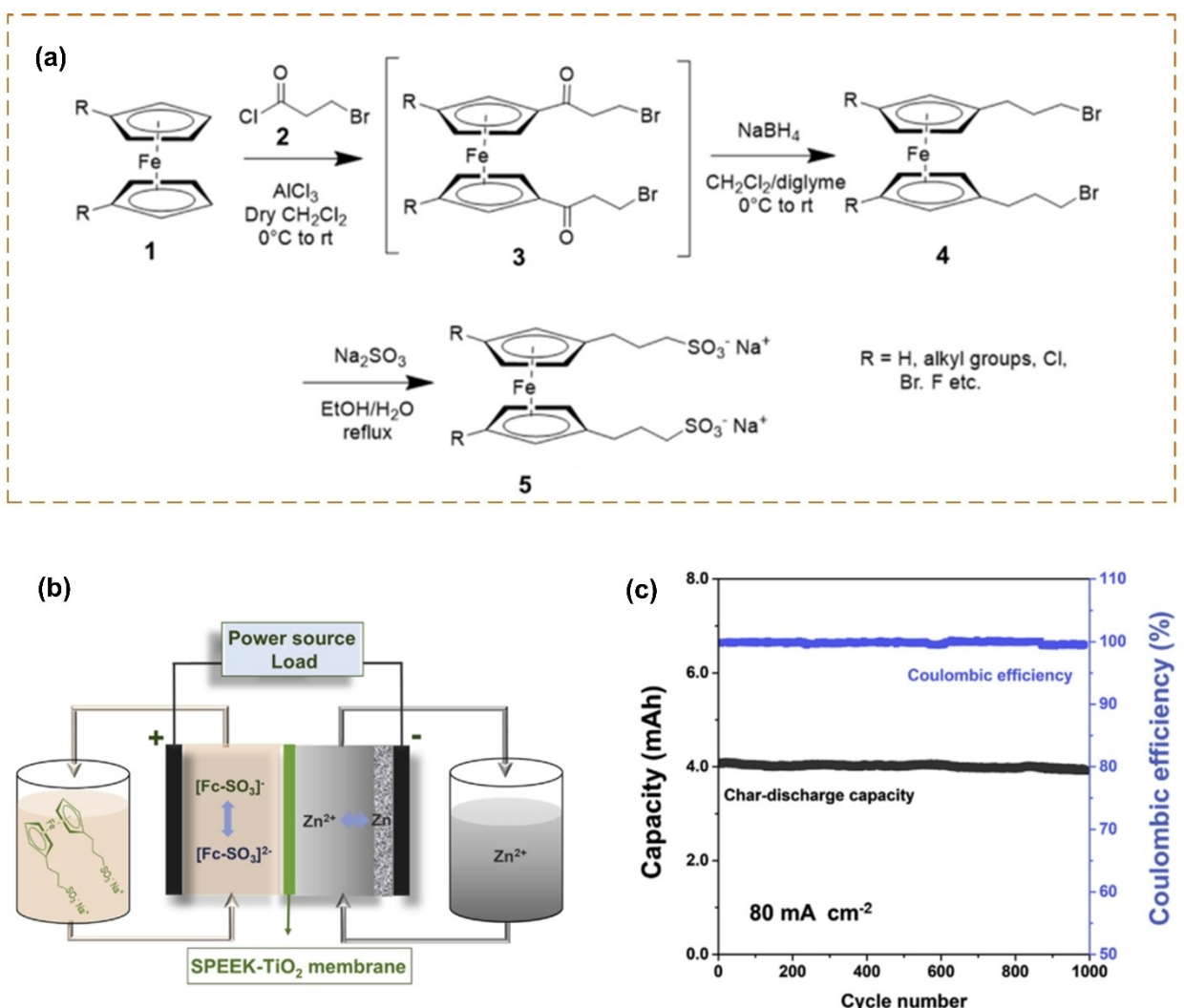


**Figure 3.** a) Synthesis route of  $\text{Fc}-\text{SO}_3\text{Na}$  and derivatives, b) Illustration of a pH-neutral aqueous redox flow battery with  $\text{Fc}-\text{SO}_3\text{Na}$  as the redox species in catholyte and Zn metal as the anode, c) Cycling performance of the battery (10 mL 21 mM  $\text{Fc}-\text{SO}_3\text{Na}$  in catholyte, 1 M  $\text{ZnSO}_4$  in anolyte with 0.5 M  $\text{Na}_2\text{SO}_4$  as supporting electrolyte) at  $80 \text{ mA cm}^{-2}$ . Adapted with permission from Ref. [76] Copyright (2020) Elsevier B.V. All rights reserved.

the battery energy density is  $27.1 \text{ Wh L}^{-1}$  (comparable to VRFBs  $25\text{--}30 \text{ Wh L}^{-1}$ ). In addition, the research team has further improved battery performance by adding  $\text{LiFePO}_4$  to the cathode tank. The experiment found that after adding  $\text{LiFePO}_4$  to the cathode tank, the battery capacity was further increased to  $562.8 \text{ Ah L}^{-1}$ .

On this basis, YAO et al.<sup>[77]</sup> obtained ferrocene ammonium sulfonate ( $\text{Fc}-\text{SO}_3\text{NH}_4$ ) through a simple synthesis step, which is a stable sulfonated ferrocene derivative with a simple synthesis route and easy large-scale production. They used  $\text{NH}_4\text{Cl}$  solution as a supporting electrolyte, and the assembled battery was tested in a neutral environment, so corrosion to the membrane was minimal. During the test, the influence of electrolyte concentration on battery capacity attenuation was explored by changing the electrolyte concentration. The experimental results show that reducing the electrolyte concentration is beneficial in slowing down the capacity retention rate of the battery during the charge-discharge cycle, which is not found in

the test of ferrocene derivatives as cathode materials reported in the previous literature. According to the team's experimental results, the solubility of  $\text{Fc}-\text{SO}_3\text{NH}_4$  in  $\text{NaCl}$  is higher than that in  $\text{NH}_4\text{Cl}$ . Therefore, they tried to use the mixed solution of 0.5 M  $\text{NaCl}$  + 0.5 M  $\text{NH}_4\text{Cl}$  as the supporting electrolyte and found that the battery could ensure a high theoretical capacity in the mixed solution. At the same time, the battery has a high capacity retention rate (in 100 charge and discharge cycles, the charging capacity is reduced by 10.35%, and the DC is only reduced by 7.45%).

Montero et al.<sup>[78]</sup> assembled a neutral aqueous organic flow battery using ferrocene 1,1-disulfonic disodium salt (DS-Fc) as the cathode electrolyte, 1,1'-bis(3-sulfonatopropyl)-viologen (BSP-Vi) and Bis(3-trimethylammonium)propyl viologen tetrachloride (BTMAP-Vi) as the anode electrolyte, respectively. These two anode electrolytes have excellent redox potential, good diffusion coefficient and good transfer rate constant. Thus, AORFBs based on BTMAP-Vi/DS-Fc and BSP-Vi/DS-Fc

redox pairs have high voltage (1.2 V and 1.3 V, respectively) and theoretical energy density ( $13 \text{ Wh L}^{-1}$ ,  $14 \text{ Wh L}^{-1}$ , respectively). It can last 70 charge and discharge cycles, and the EE is up to 97%.

The hydrophilicity and electron absorption effects of the benzenesulfonic acid group can cooperate to optimize the water solubility and redox potential of Ferrocene. FANG et al.<sup>[79]</sup> obtained sodium m-phenylferrocene sulfonate BASFc by introducing a benzenesulfonate group into the ferrocene structure through a mature diazotization reaction. The research team systematically studied the physical structure and electrochemical properties of BASFc and verified the feasibility of applying BASFc as a cathode electrolyte to AORFBs by assembling half and full batteries. The results show that the solubility of BASFc in  $\text{H}_2\text{SO}_4$  aqueous solution is close to 1.0 M, and it has good electrochemical reaction kinetics and reversibility. They assembled a full battery with 0.3 M BASFc as the cathode, 0.3 M  $\text{V}^{3+}$  as the anode, and 1 M  $\text{H}_2\text{SO}_4$  as the supporting electrolyte. The experimental results show that at  $60 \text{ mA cm}^{-2}$ , the CE is close to 100%, the EE is more than 70%, and the capacity retention rate is about 87.64% after 120 consecutive charging and discharging times. However, the attenuation mechanism of battery performance still needs to be further studied, and the matching of diaphragm and electrode materials also needs to be discussed in detail in future work to improve battery performance further.

#### 4.2. Boron Tetrafluoride is Conjugated with Ferrocene

Due to the poor chemical stability of redox raw materials, the capacity loss has been observed in almost all battery experiments, and the capacity loss mechanism of newly developed battery systems has been studied less.<sup>[80]</sup> It is common to attribute battery capacity loss to the chemical instability of the redox active materials, and while this conclusion is justified in some studies, the lack of systematic investigation in others makes it challenging to assess the stability of the proposed redox raw material critically. If we can understand the mechanism behind battery capacity loss, we can make some efforts to reduce battery capacity loss to a certain extent.<sup>[81]</sup> K.E. Tonhill et al.<sup>[82]</sup> investigated the chemical model of a simple ferrocene/ferrocenium ion ( $\text{Fc}/\text{FcBF}_4$ ) redox couple as a non-aqueous redox flow battery. Ferrocene and  $\text{FcBF}_4$  can be bought in the market, with low cost, low toxicity and other advantages, this low-cost chemical model is convenient for follow-up researchers to continue research. They use a "single redox couple cycling" in which only the  $\text{Fc}/\text{FcBF}_4$  redox pair performs the battery cycle (Figure 4a). The test results show that ferrocene has a high capacity retention rate at a concentration of 10 mM, with a capacity retention rate of up to 80% after 200 cycles (7.8 days) (Figure 4d). They found that the mechanism of capacity loss occurs through  $\text{FcBF}_4$  decomposition in the electrolyte, which is independent of the battery cycle. This work highlights the importance of studying volume

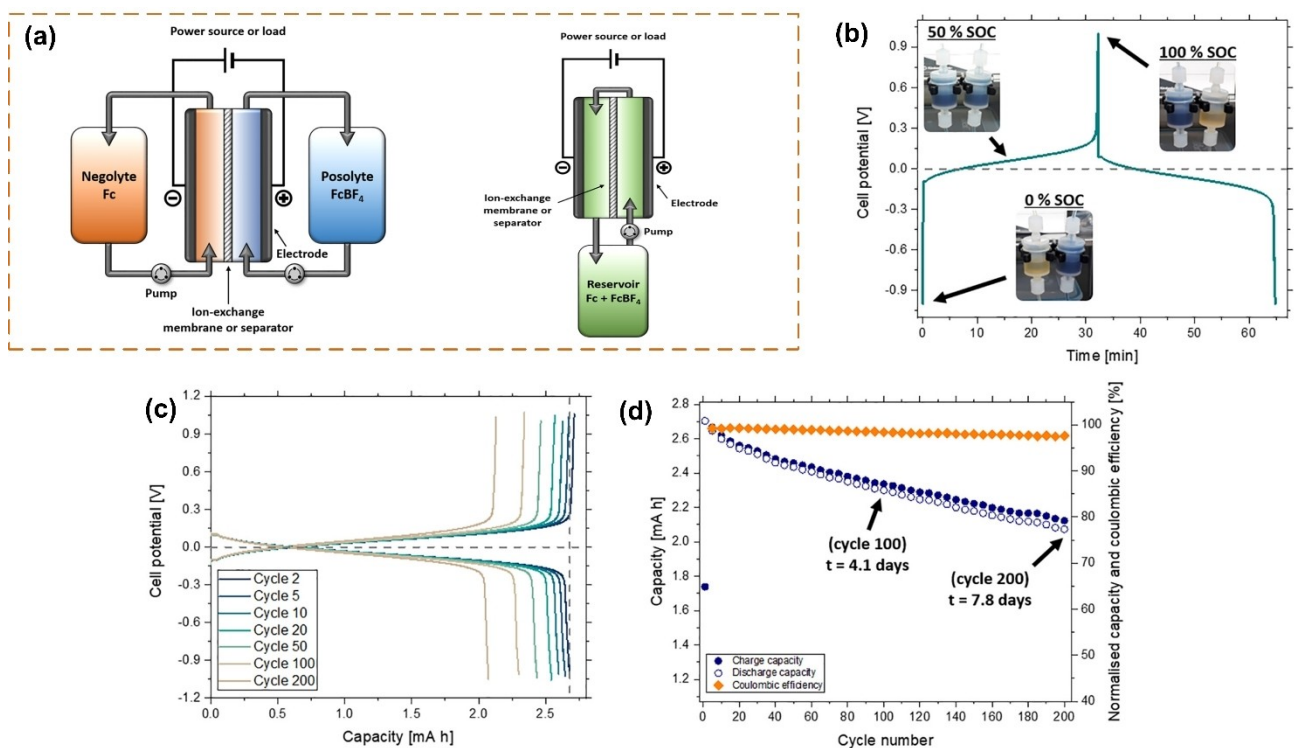


**Figure 4.** a) Schematic illustration of a RFB employing  $\text{Fc}/\text{FcBF}_4$  assembled in single redox couple configuration (left) and steady state configuration (right), b) Typical charge-discharge curve of the  $\text{Fc}/\text{FcBF}_4$  flow battery. Photographs are shown of the electrolyte reservoirs at 0, 50 and 100% SOC, c) Selected charge-discharge curves during battery cycling. The vertical dashed line indicates the 2.68 mA h capacity, d) Capacity and coulombic efficiency as a function of cycle number (battery cycled from an initial SOC of 50%). 5 mM  $\text{Fc}/\text{FcBF}_4$ , 0.1 M  $\text{TEABF}_4$ , MeCN electrolyte at  $10 \text{ mL min}^{-1}$ ,  $2.40 \text{ mA cm}^{-2}$  (1.87 C). Adapted with permission from Ref. [82] Copyright (2020) Elsevier B.V. All rights reserved.

loss in novel RFBs, as even simple redox raw materials can exhibit complex chemical reactivity. In addition, this paper also discusses the diagnostic methods of battery capacity loss. Because the cyclic voltammetry test time is usually short, it is not enough to evaluate the stability of the electrolyte. Long-term cyclic charge and discharge experiments in flow batteries should be used as a more stringent test method for capacity loss.

### 4.3. Ferrocene-Based Polymer Compounds

Schubert et al.<sup>[83]</sup> recently obtained a new type of stable aqueous redox flow battery (RFBs) electrolyte. This is a more environmentally friendly, acid-free RFBs system that can operate stably under high-temperature conditions, suitable for potential applications in Africa, India, and other high-temperature regions. They synthesized Water-soluble and ferrocene-containing methacrylamide copolymers with different comonomer ratios of the solubility-promoting comonomer [2-(methacryloyloxy)-ethyl]-trimethylammonium chloride (METAC). By studying the electrochemical properties of the polymer, using cyclic voltammetry and rotating disk electrode (RDE) method, the diffusion coefficient and charge transfer rate were obtained. The polymer was further tested in a redox flow battery device. Pairing with bis(trimethylammoniumpropyl)-viologen for charge and discharge experiments showed that the polymer exhibited a high EE of > 99.8% and good capacity retention at both room temperature and 60 °C. Detailed data showed that the selected redox couple was not only stable but also enhanced in performance at high temperatures. Furthermore, since size exclusion membranes can retain the polymer, it has the potential to replace expensive ion-selective membranes in RFBs, significantly reducing the cost of the stack. On this basis, to address the issue of low solubility of the copolymer in aqueous solutions, Schubert et al.<sup>[84]</sup> synthesized 2-ferrocenyl-ethyl methacrylate (FEMA) and its polymer through a simple method. The polar monomer SBMA can promote water solubility, and they used SBMA to synthesize the first batch of p(FEMA-co-SBMA) P3 and conducted electrochemical studies. Electrochemical characterization results showed that the charging voltage of both P3 and BTMAPV materials was approximately 1.0 V, and the discharge voltage was approximately 0.8 V. The research team also charged the battery to 0.6, 0.8, 1.0, and 1.2 V at a current of 5 mA, and the results showed a maximum capacity of 28.4 mAh at 1.0 V. In addition, to further investigate the properties of electrolyte materials, they utilized the previously discovered charging limit and charged the battery at a current of 1.0 mA, achieving a maximum average charge capacity of 29.5 mAh, which represents the maximum actual capacity of the battery. The charged RFBs were placed in an open circuit (OC) for 24 hours while continuously pumping the electrolyte. Discharging the battery demonstrated the stability of the charged material. In this test, the charge capacity decreased by approximately 0.17 mAh d<sup>-1</sup>, with an average of 95% of the electricity recovered per 24 hour discharge. To examine the survivability of the battery under more extreme

conditions, the electrolyte tank was placed in a sand bath tempered at 60 °C. The same experiment was repeated using the same battery and electrolyte. Similarly, the material was charged, and the battery was left at room temperature for 24 hours while the electrolyte was pumped through the battery, and the reservoir was heated to 60 °C. The charge capacity decreased by 0.69 mAh d<sup>-1</sup>, but an average of 87% of the electricity was recoverable, which was much lower than the data obtained from the previous open circuit (OC) experiment. This indicated that the higher the temperature of the battery setup, the faster the performance of the active materials would decline. This study expanded the understanding of the synthesis, solid-state structure, and polymerization behavior of ferrocene-containing monomers and provided the first in-depth exploration of their application in RFBs. This made them highly competitive compared to other polymer systems reported so far.

### 4.4. Using Dimethylamine Functional Ferrocene as Raw Material

#### 4.4.1. Symmetrical NORFBs of Ferrocene/O-Phenylenediamine Ions

Conventional RFBs are affected by electrolyte crossing due to the different concentrations of the two redox pairs on the diaphragm. Therefore, it is prone to self-discharge, low CE, complex side reactions and capacity attenuation between mixed redox electric pairs.<sup>[85]</sup> In contrast, symmetrical NARFBs using bipolar redox active organic molecules (BROMs) as cathode and anode active materials have received increasing attention due to the simpler type of redox active materials in the electrolyte.<sup>[86]</sup> A series of ionic BROMs based on ferrocene (Fc) and phthalimide (Ph) moieties with fast mass and charge-transfer kinetic are synthesized by Xu et al.<sup>[87]</sup> and they have excellent electrochemical properties. On this basis, they synthesized a series of ionic brominated materials based on ferrocene and Ph. The solubility of FcPh in 1,3-dioxolane (1,3-DL) is only 0.64 M, and the current density of FcPh-based H-type coin batteries is also low (0.04 mA cm<sup>-2</sup>). FcPh has introduced as an ionic-charged tetraalkylammonium moiety with a bis(trifluoromethylsulfonyl)imide anion (TFSI<sup>-</sup>), leading to the relatively high solubility of up to 2.27 M in N,N-dimethylformamide (DMF) and inherent ionic conductivity. FcnPh-TFSI (n=2, 4, and 6) with different chain lengths of 2,4, and 6 carbons between the Ph moiety and quaternary nitrogen atom were synthesized. The experimental results show that at least n=4 is required to obtain stable electrochemical properties. The Fc4Ph-TFSI based flow battery can cycle 50 times under the condition of 20 mA cm<sup>-2</sup>, the OCV is 2.04 V, CE is 94.6%, EE is 77.0%, the capacity retention rate of each cycle is 99.8%, and the peak power density is 110 mW cm<sup>-2</sup>. It is more competitive than NARFBs reported so far. In addition, the research team found that the acidity of the solvent can affect the stability of organic free radical ions, thus affecting the cyclic stability of the flow battery. Both the calculated and experimental results show

that the chain length and the acidity of the solvent play a key role in the cycle stability of the battery.

#### 4.4.2. Ferrocene Containing Dimethylamine as a Cathode Electrolyte

Christopher J. Ziegler and his colleagues synthesized a series of "all-ferrocene" salts and investigated their electrochemical activities.<sup>[88]</sup> The four salts are formed via metathesis reactions employing the (ferrocenemethyl)trimethylammonium cation and mono and bis sulfonate or carboxylate ferrocene anions. Systems composed of multiple ferrocene units can exhibit multiple redox potentials due to different substitutions on the ferrocene units. Therefore, it is theoretically possible to achieve a stable mixed-valence state and obtain electrical potential from reactions between the fully oxidized and fully reduced forms, such as the diferrrocene system. They altered the stoichiometry of ferrocene ions by using mono- or functionalized ferrocenes and studied the ferrocene salts and their anion and cation precursors using electrochemical methods. It's worth noting that the redox potentials of the ions in Salts 1–4 are highly dependent on solvent conditions. A comparison was made by dissolving them in water, PC, and DMF. The results indicate that, besides other solvent interactions, hydrogen bonding may play a critical role in regulating the redox potentials of the anionic components of these salts. This effect is particularly significant in salts containing bis(sulfonate anions). Apparently, the choice of solvent and ferrocene ions will play a crucial role in any redox flow battery design. For RFBs materials, the system with the largest potential difference between ferrocene cations and anions is Compound 3. This salt can form a stable mixed-valence state depending on the choice of solvent. It's worth mentioning that ferrocene sulfonates have better solubility than ferrocene methanol and are reversible. This is the first evaluation of the possible energy storage applications of these compounds. Certainly, further research on these compounds and the influence of solvents and solvation on potentials is necessary.

#### 4.4.3. Bromine Ligand Ferrocene Derivatives for ORFBs

An important performance aspect of using organic redox couples for aqueous redox flow batteries (RFBs) is the ability to obtain charge storage materials with the highest concentration and reversibility.<sup>[89]</sup> Jeon et al.<sup>[90]</sup> prepared Fc1 N112-Br by nucleophilic substitution of dimethylaminomethyl ferrocene ( $C_{13}H_{17}FeN$ ) with bromoethane ( $C_2H_5Br$ ) in acetonitrile ( $C_2H_3CN$ ) and used it as the cathode electrode part for ORFBs. Experiments have confirmed that Fc1 N112-Br exhibits excellent electrochemical performance, including high solubility above 2.9 M (72 times higher than unsubstituted Ferrocene), nearly equal diffusion coefficients for  $Fe^{2+}$  and  $Fe^{3+}$ , charge transfer coefficient close to 0.5, and significantly improved reaction kinetics. Therefore, Fc1 N112-Br is not only electrochemically stable and reversible but also quasi-reversible and symmetrical

in redox reactions. They used nuclear magnetic resonance (NMR), cyclic voltammetry (CV), and linear sweep voltammetry (LSV) analyses to confirm the solubility, stability, electrochemical reversibility, and kinetic rate of Fc1 N112-Br in aqueous solution, thereby demonstrating its chemical and electrochemical properties. Battery cycle test results showed that the charge transfer coefficient of Fc1 N112-Br was close to 0.5 in 0.5 M, 1.0 M, and 1.5 M Fc1 N112-Br electrolytes, indicating that the redox reaction of Fc1 N112-Br is quasi-reversible and symmetrical. Additionally, battery operation results showed a CE of 95.7% using Fc1 N112-Br (Figure 5a).

#### 4.4.4. $FcNCl$

The widespread application of conventional RFBs such as vanadium and Zn–Br RFBs is limited by a number of material challenges, including low abundance and high cost of redox active metals, expensive separators, active materials crossing, and corrosive and harmful electrolytes.<sup>[91]</sup> To address these challenges, LIU et al.<sup>[92]</sup> demonstrated a neutral aqueous water-based organic redox flow battery (AORFBs) technology that utilizes a newly designed cathode electrolyte that contains highly water-soluble ferrocene molecules. By modifying the structure of hydrophobic Ferrocene, they synthesized water-soluble (ferrocenylmethyl)-N<sup>1</sup>, N<sup>1</sup>, N<sup>2</sup>, N<sup>2</sup>, N<sup>2</sup>-pentamethylpropane-1,2-diaminium dibromide ( $FcN_2Br_2$ ) (Figure 5b). The two AORFBs,  $FcNCl/MV$  and  $FcN_2Br_2/MV$ , can operate in a non-corrosive neutral NaCl electrolyte using a low-cost anion exchange membrane when paired with MV as an anode electrolyte. These  $Fc/MV$  AORFBs have a high theoretical energy density (45.5 Wh L<sup>-1</sup>) and excellent cyclic performance in the range of 40 mA cm<sup>-2</sup>–100 mA cm<sup>-2</sup> (Figure 5c and d). Notably, the  $FcNCl/MV$  AORFB (7.0 and 9.9 Wh L<sup>-1</sup>) demonstrated unprecedented long-cycle performance, with 700 cycles at 60 mA cm<sup>-2</sup>, a capacity retention rate of 99.99% per cycle, and a power density of up to 125 mW cm<sup>-2</sup>. LIU et al.<sup>[93]</sup> further proposed three ferrocene cathode electrolytes  $C_1$ - $FcNCl$ ,  $C_2$ - $FcNCl$  and  $C_3$ - $FcNCl$  in the follow-up work. Their physicochemical and electrochemical properties, battery properties and degradation mechanism in pH-neutral aqueous solution were investigated. UV-Vis and gas chromatography (GC) studies confirmed the ligand dissociation and decomposition pathway of the  $C_x$ - $FcNCl$  cathode under electrolyte discharge and charged state. In the  $C_3$ - $FcNCl$  cathode electrolyte, the electron-donating 3-(trimethylammonium) propyl group strengthens the  $C_3$ -Cp ligand and the  $Fe^{3+}$  or  $Fe^{2+}$  center, thereby alleviating ligand dissociation degradation. Based on the above experimental results, the ferrocene electrolyte showed cyclic stability in half battery and full battery flow batteries, in the order of  $C_1$ - $FcNCl$  >  $C_2$ - $FcNCl$  >  $C_3$ - $FcNCl$ . Under neutral conditions, the most stable  $C_3$ - $FcNCl$  is in 0.50 M ORFB at 10 mA cm<sup>-2</sup>, with a capacity retention rate of 99.998% per cycle, or 99.927% per day for 500 cycles (Figure 5e).

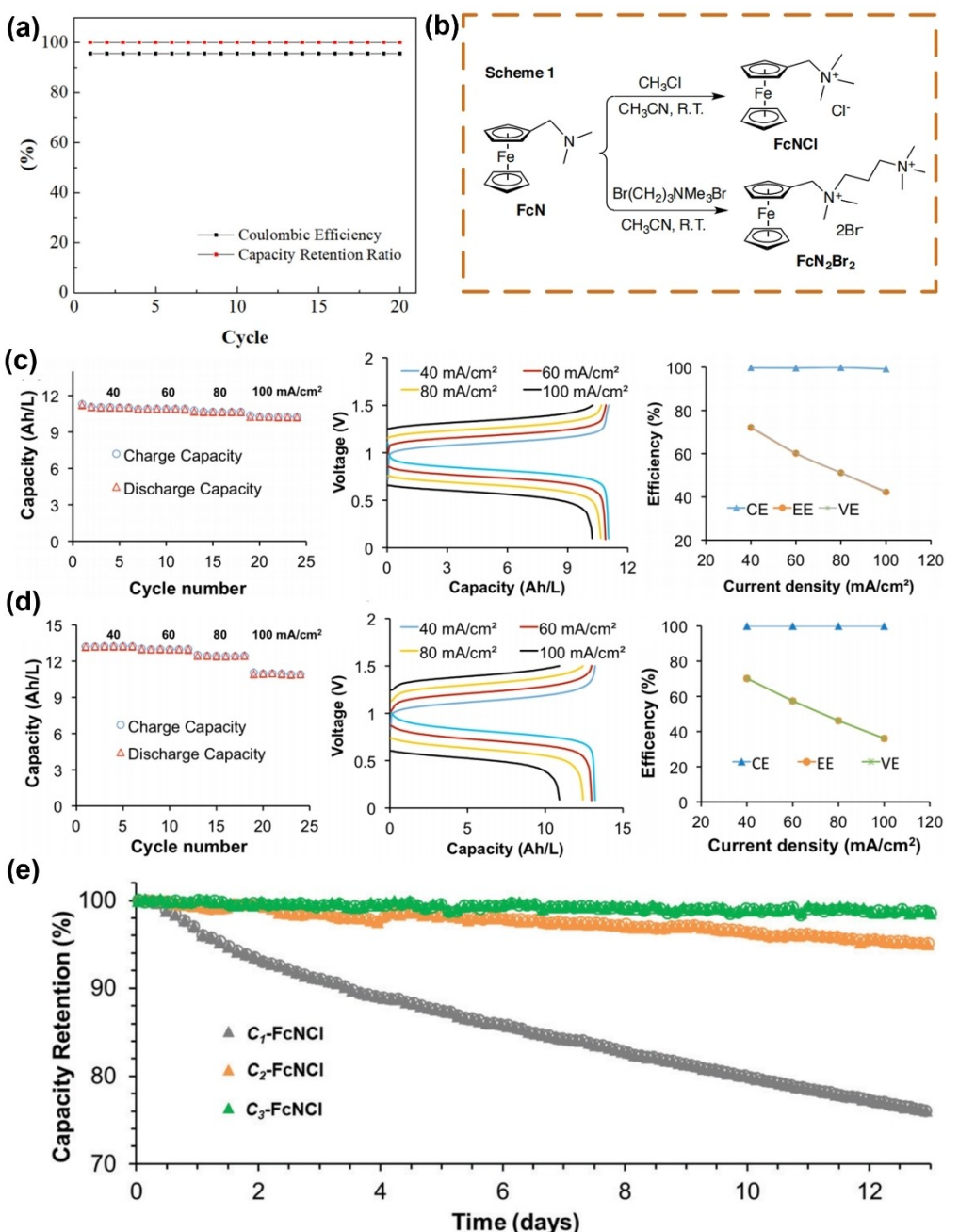


**Figure 5.** a) Discharge capacity retention ratio and coulombic efficiency curves, b) Synthetic routes for FcNCl and FcN<sub>2</sub>Br<sub>2</sub>, c) Cycling performance of FcNCl/MV AORFB, d) Cycling performance of FcN<sub>2</sub>Br<sub>2</sub>/MV AORFB. Adapted with permission from Ref. [91] Copyright (2016) American Chemical Society. e) Capacity retention of 0.50 M C<sub>x</sub>-FcNCl half-battery RFBs at 40 mA cm<sup>-2</sup> during 13 testing days: C<sub>1</sub>-FcNCl (gray), C<sub>2</sub>-FcNCl (orange), and C<sub>3</sub>-FcNCl (green). Adapted with permission from Ref. [93] Copyright (2022) The Royal Society of Chemistry.

#### 4.4.5. Zwitterionic Ferrocene: A Method for Cathodes of RFBs

EunsungLee et al.<sup>[94]</sup> recently synthesized the imidazolium-/pyrrolinium-substituted persistent zwitterionic ferrocene derivatives. They were characterized by electron paramagnetic resonance (EPR) and <sup>57</sup>Fe Mössbauer spectroscopy, and by simple Fe(II/I) redox chemistry, it was successfully demonstrated that the pyrrolinium-substituted ferrocene derivative could be used as active materials in redox flow batteries (Figure 5a and b). At 20 mA cm<sup>-2</sup>, the charge-discharge curve shows an

average battery voltage of 1.40 V (Figure 6c), which is consistent with cyclic voltammetry data. Notably, the initial capacity of 0.62 Ah L<sup>-1</sup> is fairly close to the theoretical capacity of 0.80 Ah L<sup>-1</sup>, indicating a material utilization rate of ~78%. Cycle efficiency and capacity retention data for the battery show that the flow battery maintained up to 99% CE, 71% VE, and 70% acceptable EE for 50 cycles (Figure 6d). This study shows that highly unstable ferrocene derivatives can not only be stabilized in the form of ferrocene oligomers but can also be further used as solutes in redox flow batteries. These ferrocene derivatives

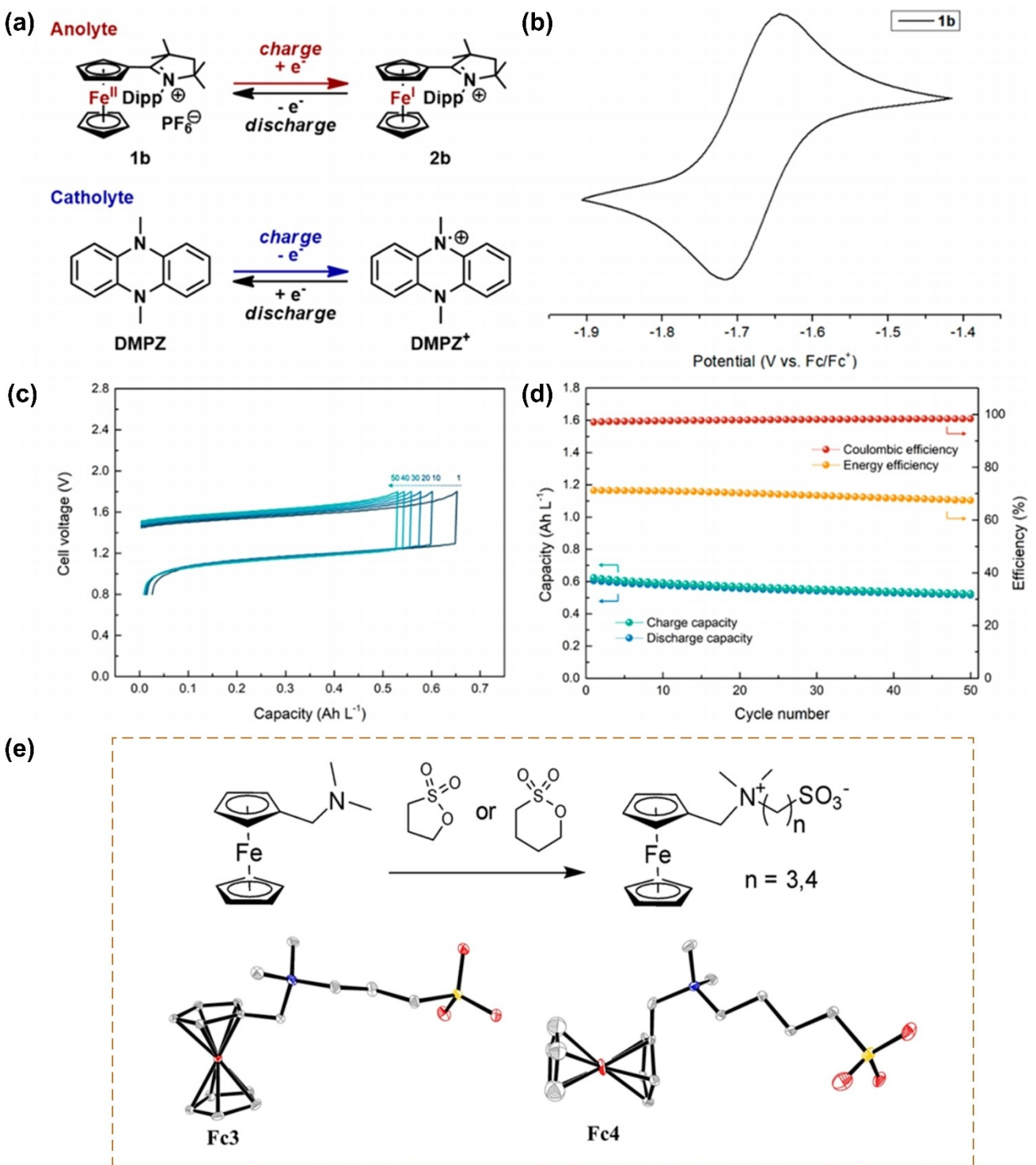


**Figure 6.** a) Redox mechanism of 1b and DMPZ in a flow battery, b) Cyclic voltammogram of 1b in 0.5 M LiTFSI/MeCN (vs Fc/Fc<sup>+</sup>, scan rate = 0.1 V s<sup>-1</sup>) Charge – discharge curves for 1, 10, 20, 30, 40, and 50 cycles, d) Cycling efficiencies and capacities with 50 cycles. Adapted with permission from Ref. [93] Copyright (2021) American Chemical Society. e) Synthesis and single-crystal X-ray structures of zwitterionic ferrocenes Fc3 and Fc4 with 35 % thermal ellipsoids. Adapted with permission from Ref. [95] Copyright (2022) American Chemical Society.

deepen our understanding of the electrochemical behavior of ferrocene compounds and pave the way for the rational design of ferrocene derivatives.

Recently, Zhang et al.<sup>[95]</sup> paired new zwitterionic ferrocene derivatives, Fc3 and Fc4, with anthraquinone-2,7-disulfonate

salt (AQDS) to successfully propose an aqueous flow battery system. These compounds are prepared by reactions of propyl and butyl sultones, respectively, with dimethylaminomethylferrocene, and the resulting products are separated in the form of pure crystals. The two compounds are highly miscible with

water, and the solubility is 0.66 and 2.01 M, respectively. Since solubility, the theoretical volume capacity is calculated according to Faraday's law, which is  $17.69$  and  $53.87 \text{ Ah L}^{-1}$ , respectively.<sup>[96]</sup> These ferrocene derivatives exhibit excellent properties in neutral aqueous solutions. The VE and EE are about 88%, and the CE of the two high-concentration redox flow batteries is more than 99%. Interestingly, capacity monitoring and cyclic voltammetry of the battery showed that Fc4 had higher stability compared to Fc3. At the end of 20 cycles, the volume decreased by ~5% (~1% per day). Density functional theory calculations (DFT) were used to investigate the stability of possible conformations of two zwitterionic ferrocenes in solution. The DFT calculations show that there are significant differences in the conformational properties of Fc3 and Fc4, with Fc4 retaining the linear structure of the side chain in solution, while Fc3 prefers both linear and curved geometry (Figure 6e). The approach presented here introduces an entirely new direction for the development of water-based RFBs. In addition, the ionized approach can serve as a general guideline for designing RFBs, with improved solubility and recyclability

characteristics that are much needed for next-generation batteries.

#### 4.5. Multicore Ferrocene

Gao et al.<sup>[97]</sup> studied and synthesized ferrocene carboxylic acid Fe, Co, and Ni complexes as model complexes to investigate how many ferrocene units in a multi-ferrocenyl system can react with electrodes. They successfully synthesized complexes (1)–(3) (Figure 7a) and characterized their molecular structures using X-ray single-crystal diffraction. By comparing the cyclic voltammetry test data of Ferrocene and complexes (1)–(3) and estimating the diffusion coefficients of complexes (1)–(3) and Ferrocene using Diffusion Ordered Spectroscopy (DOSY) and the Einstein–Stokes equation, they calculated the number of electrode reactions for Ferrocene in complexes (1)–(3). A spherical polyferrocene electrode reaction model was established (Figure 7b). If the diameter of the spherical polyferrocene system is greater than 1 nm, the ferrocene units of the spherical

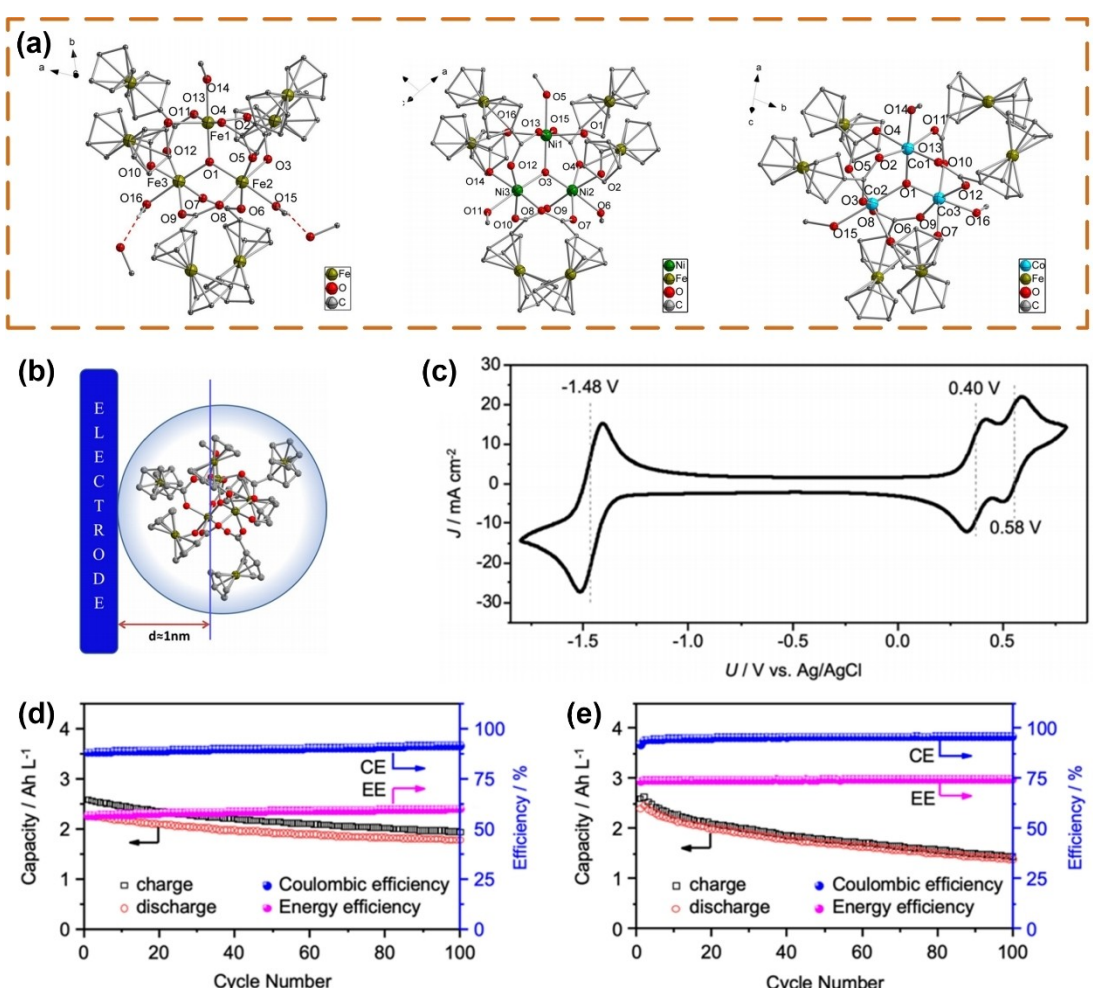


**Figure 7.** a) Molecular structure of Fe, Co, and Ni complexes, b) Contact between ferrocene complex model and electrodes. Adapted with permission from Ref.<sup>[97]</sup> Copyright (2019) Institute of Chemistry, Slovak Academy of Sciences. c) CV profiles of the acetonitrile solution containing 5 mM DFDE, 10 mM BuPh<sub>4</sub>, and 0.5 M TBABF<sub>4</sub> recorded at a scan rate of  $50 \text{ mV s}^{-1}$  with a three-electrode configuration, where a glass carbon electrode, a piece of graphite felt, and an Ag/AgCl electrode serve as the working, counter, and reference electrodes, respectively. Capacity retention and corresponding Coulombic efficiency and energy efficiency of (d) symmetric and (e) asymmetric batteries. Adapted with permission from Ref. [98] Copyright (2020) American Chemical Society.

polyferrocene system cannot completely react with the electrode. Zhao et al.<sup>[98]</sup> designed and synthesized a multicore ferrocene derivative, 4,4'-diferrocenyl-1-(2-methoxy-ethoxy)-pentane (DFDE), as a highly soluble cathode active material for NARFBs. This research group demonstrated the use of multicore ferrocene derivatives as electrolyte materials for ORFBs for the first time. Due to the customized ether chain and the synergistic effect of multiple ferrocene cores, DFDE has a high solubility of 4.5 M equivalent electronic concentration in ether-based solvents and a higher positive redox potential compared to the original Ferrocene, which is crucial for improving the energy density of NARFBs. Combined experimental and DFT simulation studies provide a molecular-level understanding of intermolecular forces and solvation chemistry in customized ferrocenes. Additionally, electrochemical characterization indicates that DFDE undergoes highly reversible redox reactions with a fast electron transfer rate constant. When paired with N-butyl-phthalimide (BuPh), the battery has a discharge voltage of approximately 1.8 V (Figure 7c) and stable cycling performance (Figure 7d and e). The capacity based on 1 M DFDE cathode material reaches 36.7 Ah L<sup>-1</sup>, which is comparable to the current state-of-the-art aqueous system. The results suggest that it is a feasible strategy to improve the performance of ferrocene-based complexes using molecular structure engineering techniques while maintaining a tolerable environmental and ecological load.

#### 4.6. Study of Ferrocene in Microemulsions Such as Butanol

Shen et al.<sup>[99]</sup> recently proposed a microemulsion that could be used as an alternative electrolyte for RFBs. Microemulsions can not only dissolve redox active materials that are incompatible with water, potentially increasing energy density but also provide the high conductivity of water-salt electrolytes. They demonstrated this concept by studying the transport of ferrocene in a toluene/Tween 20/1-butanol/water model microemulsion. Ferrocene is stored in the toluene phase as the redox material, showing rapid electron transfer, which suggests a promising approach for RFBs. The results indicate that ferrocene is redistributed in the oil microenvironment, surfactant microenvironment, and water microenvironment, with corresponding diffusion coefficients and partition coefficients quantified. Therefore, they proposed a tortuous path diffusion model to describe the mass transfer process of ferrocene to the electrode surface. Diffusion coefficients can also be obtained through PFG-NMR, but the ferrocene diffusion values are significantly higher than those measured electrochemically, indicating differences in how they measure samples. Data on the current contribution of each microenvironment suggests that although electron transfer reactions may occur in surfactants, the permeability of ferrocene in oil is much higher.

### 5. Other Metal Complexes are used for Organic RFBs

#### 5.1. MCCs Based on Bipyridine

The first MCC to be considered as an active species in NARFBs was [Ru(bpy)<sub>3</sub>]<sup>2+</sup> in 1988 by Matsuda et al.<sup>[100]</sup> A new type of redox battery was developed by using ruthenium complexes in organic electrolyte solution as the electrode active materials. In acetonitrile solution, a single battery composed of [Ru(bpy)<sub>3</sub>]<sup>2+</sup> has an open circuit voltage of 2.6 V (Figure 8b) and a discharge current of 5 mA cm<sup>-2</sup> (on a smooth carbon electrode). The characteristics of such batteries are greatly affected by factors such as the membrane material and the concentration of the compound. Thompson et al.<sup>[101]</sup> developed a series of ester-functionalized chromium bipyridine complexes (Figure 8c), which they found to have enhanced solubility in different oxidation states. These chromidopyridine complexes have been shown to provide up to six reversible redox couples (Figure 8d) with a solubility of close to 1 M in excess of 2 V. Using an electrolyte consisting of tris(4,4'-bis(2-(2-methoxyethoxy)-ethyl)ester)-2,2'-bipyridine)chromium complex ([Cr(L3)<sub>3</sub>]) in acetonitrile. They assembled a symmetric H-battery for testing (Figure 8e). The results showed two reversible electron transfers at each electrode, with an efficiency of 70%. The solubility of the active materials in the organic electrolyte directly affects the energy density of the battery to a large extent. Mun et al.<sup>[102]</sup> used bis(trifluoromethanesulfonyl)imide (TFSI) as the antianion of the complexes of iron and nickel tris(2,2'-bipyridine) ((Bpy)<sub>3</sub>) as the active material in high-energy RFBs. The synthetic salts were characterized by nuclear magnetic resonance (NMR), inductively coupled plasma mass spectrometry (ICP-MS) and electrochemical analyses. They also found that Ni(Bpy)<sub>3</sub>(TFSI)<sub>2</sub> and Fe(Bpy)<sub>3</sub>(TFSI)<sub>2</sub> containing bulky imide anions weakened the inter-anion Coulombic interactions via charge delocalization, thereby increasing the solubility. Thanks to the excellent electrochemical stability of this electrolyte, redox flow batteries can operate at voltages higher than 2.1 V.

#### 5.2. Tridentate Nitrogen Donor Ligand (Tripyridine) Complexes

In 2018, Yang et al.<sup>[103]</sup> found that [Co(bpy)<sub>3</sub>]<sup>2+</sup> charged near 1.31 V potential in symmetrical RFBs and maintained 82% capacity after 25 cycles. The cycling performance of Li/Co-complex redox batteries was examined at a current density of 0.5 mA cm<sup>-2</sup>. After 20 cycles, the capacity retained 99.9%, 99.7%, and 99.1% for Co(L1)<sub>3</sub>, Co(L2)<sub>2</sub>, and Co(L3)<sub>2</sub>, respectively, in diglyme and 99.7% for Co(L3)<sub>2</sub> in EC-DMC (Figure 9a-d). The CE of all co-complexed cathode electrolytes was maintained at about 99.9%, indicating that there was no significant effect on the electron transfer rate in the current density that these batteries were able to deliver. This significant capacity retention and CE indicate that the co-complex is stable in the Co (II/III) repeat cycle. Toghill et al.<sup>[104]</sup> reported a single species redox

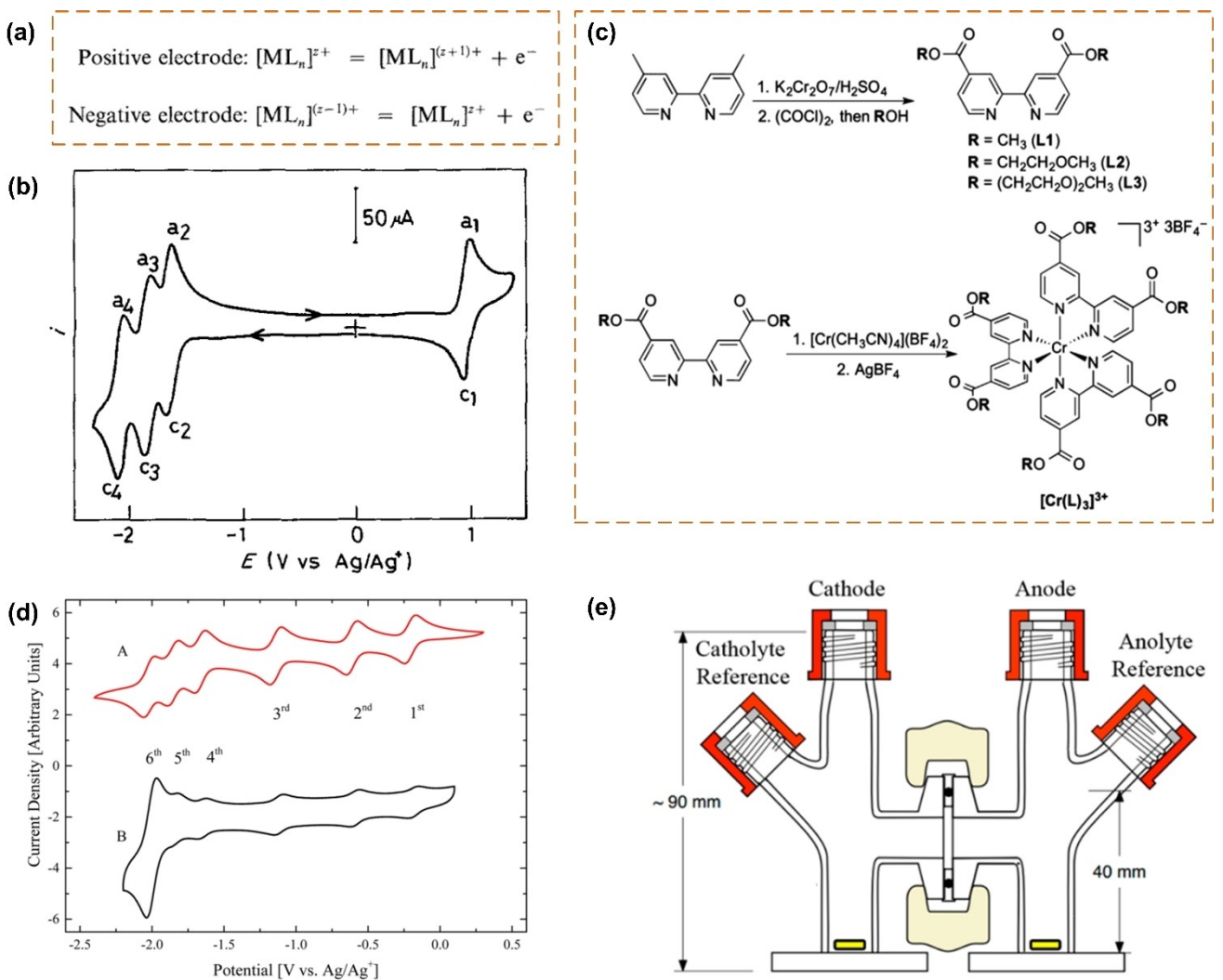


**Figure 8.** a) The principle of the battery is indicated in Equation 1, b) Cyclic voltammogram of  $[\text{Ru}(\text{bpy})_3](\text{BF}_4)_2$  at GC electrode in  $\text{Et}_4\text{NBF}_4$  (0.1 M)/CH<sub>3</sub>CN. Concentration of  $[\text{Ru}(\text{bpy})_3](\text{BF}_4)_2 = 2 \times 10^{-3}$  mol dm<sup>-3</sup>, electrode area = 0.096 cm<sup>2</sup>, potential scan rate = 0.3 V s<sup>-1</sup>, temperature = 30 °C. Adapted with permission from Ref. [100]. Copyright (1988) Chapman and Hall Ltd. c) Synthesis of 4,4'-Ester-Substituted Bipyridine Ligands L1, L2, and L3 and Synthesis of Functionalized  $[\text{Cr}(\text{L})_3]^{3+}$  Complexes, (d) Cyclic voltammograms for (A) 1 mM  $[\text{Cr}(\text{L}1)_3]^{3+}$  and (B) 0.48 mM  $[\text{Cr}(\text{L}1)_3]$  (saturated solution) in acetonitrile, e) Schematic of an electrochemical H- battery used for testing charge/discharge performance of flow battery active species. Adapted with permission from Ref. [101] Copyright (2018) American Chemical Society.

flow battery employing a new class of cobalt (II) complexes with ‘tunable’ tri-dentate azole-pyridine type ligands is reported. Four structures were synthesized, and their electrochemical, physical and battery characteristics were investigated as a function of successive substitution of the ligand terminal pyridyl donors. The Co (II/I) and Co (III/II) couples are stable and quasi-reversible on gold and glassy carbon electrodes. However, redox potentials are tunable, allowing the cobalt potential difference to be preferentially increased from 1.07 to 1.91 V via pyridine substitution with weaker σ-donating/II-accepting 3,5-dimethylpyrazole groups. The charge-discharge performance of the system was evaluated by using H-type glass batteries and graphite rod electrodes. The complex was found to have a CE of 89.7–99.8%, and the EE of the system was as high as 63.1–80.8% (Figure 9e), an improvement compared to other similar non-water systems. Smith et al.<sup>[105]</sup> found that the use of

$\text{CF}_3\text{SO}_3^-$  as an anion of the active salt results in more stable cycling performance than salts containing  $\text{BF}_4^-$  and  $\text{FSI}^-$  while improving the cycling performance of the redox activity  $[\text{Fe}(\text{bpy})_3]^{2+}$  cations in non-aqueous flow batteries without the need for additional supporting electrolytes. They synthesized  $[\text{Fe}(\text{bpy})_3](\text{CF}_3\text{SO}_3)_2$ , characterized it electrochemically by cyclic voltammetry, and tested it under different cyclic conditions in a symmetric flow battery. The results show that the battery can survive more than 800 cycles at a current density higher than 10 mA cm<sup>-2</sup>, which is at least a 40-fold improvement in cycle life and a 5-fold improvement in power capacity compared to studies in the literature involving similar active species. The main reason for the decline in performance may be due to the increased ohmic loss in the battery. Erasmus et al.<sup>[106]</sup> prepared five Co<sup>II</sup> complexes, and they found that the Co<sup>III/II</sup> redox couple measured in DMF ranged between -1.1 and -1.7 V vs. HFc/

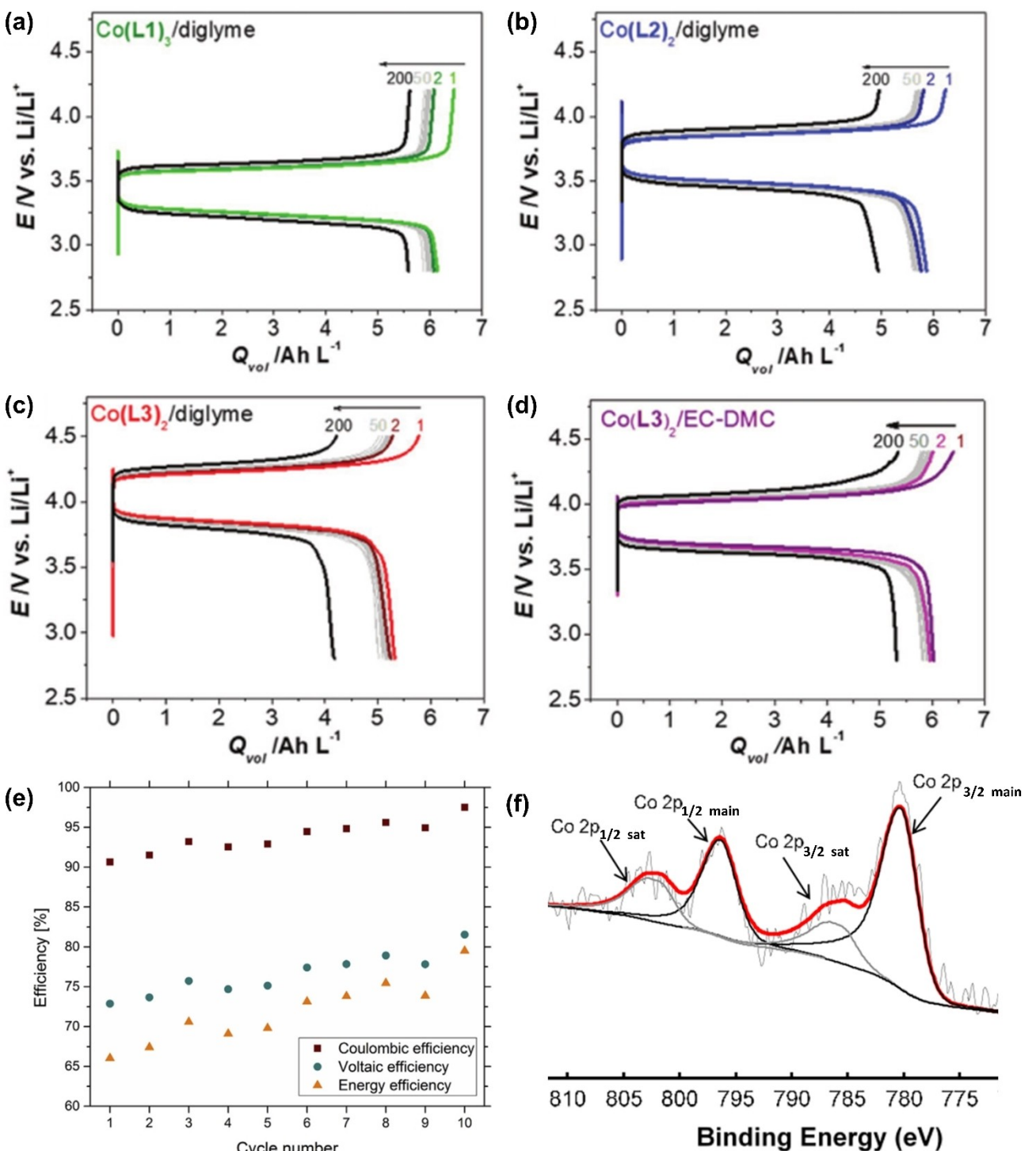


**Figure 9.** a)  $\text{Co(L1)}_3$ , b)  $\text{Co(L2)}_2$ , c)  $\text{Co(L3)}_2$  in 1 M LiTFSI/diglyme, and d)  $\text{Co(L3)}_2$  in 1 M LiTFSI/EC-DMC catholyte at a current density of  $0.5 \text{ mA cm}^{-2}$ . Adapted with permission from Ref. [103] Copyright (2018) WILEY-VCH Verlag GmbH & Co. KGaA, Weinheim. e) Battery performance as a function of cycle number of 1 mM complex 4 in 0.5 M TBA PF<sub>6</sub> MeCN solution at  $\pm 4.4 \mu\text{A cm}^{-2}$ . Squares - coulombic efficiency, circles - voltaic efficiency, triangles - energy efficiency. Adapted with permission from Ref. [104] Copyright (2017) Published by Elsevier B.V. All rights reserved. f) The survey XPS detail scans illustrating the  $\text{Co } 2p$  photoelectron lines of the XPS spectrum of the complex 3. Adapted with permission from Ref. [106] Copyright (2023) The Author(s). Published by Elsevier B.V.

$\text{HFc}^+$ . XPS test results further confirm that the Co metal center is in the II oxidation state (from the binding energy position of the  $\text{Co}2p_{3/2}$  photoelectron line) (Figure 9f). Directly proportional relationships were established between the  $E^{0'}$  of both the  $\text{Co}^{IV}$

$^{III}$  and  $\text{Co}^{III/II}$  redox couples and the BE of the main  $\text{Co}^{II} 2p_{3/2}$  photoelectron lines and DFT calculated energies and charges. These relationships all illustrate the electronic influence of the different N-donor ligands on the effective charge of the central

cobalt (II) ion the ligands are coordinated to, can be quantised by the different experimental redox and XPS BE values and DFT calculated electronic descriptors.

### 5.3. Acetylacetone-Based Complexes

Liu et al.<sup>[107]</sup> first used  $[\text{V}(\text{acac})_3]$  complex as electrolyte materials for neutral ORFBs in 2009, an early example of the application of Metal coordination complexes (MCC) as redox active materials in NARFBs. The electrochemistry of a single-component redox flow battery employing vanadium (III) acetylacetone in acetonitrile and tetraethylammonium tetrafluoroborate has been investigated by researchers.  $[\text{V}(\text{acac})_3]$  exhibits two reversible redox events in the MeCN solvent, a  $\text{V}^{\text{II}}/\text{V}^{\text{III}}$  couple at  $-1.7\text{ V}$  and a  $\text{V}^{\text{III}}/\text{V}^{\text{IV}}$  couple at  $0.5\text{ V}$  vs.  $\text{Ag}/\text{Ag}^+$ . It is allowed to be used in posolyte ( $\text{V}^{\text{III}}$  oxidized to  $\text{V}^{\text{IV}}$  on charge) and negolyte ( $\text{V}^{\text{III}}$  reduced to  $\text{V}^{\text{II}}$ ) half batteries, resulting in symmetrical RFBs with a theoretical battery potential of close to  $2.2\text{ V}$ , nearly twice that of AORFBs. Subsequently, Liu et al.<sup>[108]</sup> used electrochemical technology to study the monumental redox flow battery prepared from chromium (III) acetylacetone in tetraethylammonium tetrafluoroborate and acetonitrile. Although applications of chromium complexes in water-based RFBs have been reported before, this is their first application in monometallic non-water-based RFBs. They evaluated the electrode kinetics of the complex by cyclic voltammetry and observed that there were four redox pairs in the stable potential window, namely  $\text{Cr}^{\text{II}}/\text{Cr}^{\text{III}}$ ,  $\text{Cr}^{\text{I}}/\text{Cr}^{\text{II}}$ ,  $\text{Cr}^{\text{III}}/\text{Cr}^{\text{IV}}$ , and  $\text{Cr}^{\text{IV}}/\text{Cr}^{\text{V}}$ . All four sets of redox pairs are quasi-reversible, in which the  $\text{Cr}^{\text{III}}/\text{Cr}^{\text{IV}}$  pairs exhibit relatively slow kinetics. The results of cyclic voltammetry show that the  $\text{Cr}(\text{acac})_3$  complex can be oxidized to  $[\text{Cr}(\text{acac})_3]^{+}$  and  $[\text{Cr}(\text{acac})_3]^{2+}$  and reduced to  $[\text{Cr}(\text{acac})_3]^-$  and  $[\text{Cr}(\text{acac})_3]^{2-}$  on the glass carbon electrode. The charging and discharging characteristics of the H-type glass battery were evaluated by a membrane separator. In an electrolyte containing  $0.05\text{ M}$   $\text{Cr}(\text{acac})_3$  and  $0.5\text{ M}$   $\text{TEABF}_4$ , the CE and EE of the battery during the cycle from 0 to 50% of the theoretical maximum SOC are 53–58% and 21–22%, respectively. The concentration of active materials limits the energy density of redox flow batteries. At present, the solubility of chromium acetyl acetone in acetonitrile reported by the research team at room temperature is  $\sim 0.4\text{ M}$ , so it is necessary to study the modification of ligands and solvents to increase the solubility of active materials.

To investigate the effect of electrode type on the rate of oxidation and reduction of vanadium acetylacetone in tetraethylammonium tetrafluoroborate and acetonitrile electrolytes, Monroe et al.<sup>[109]</sup> dissolved vanadium acetylacetone in tetraethylammonium tetrafluoroborate and acetonitrile, and three electrode materials (glassy carbon, gold, and platinum) were tested using cyclic voltammetry and linear scanning voltammetry to determine the coulombic of the oxidation and reduction of  $\text{V}(\text{acac})_3$  on each material reversibility, kinetic reversibility and exchange current density. Cyclic voltammetry results show that the peak-to-height ratio of all redox pairs and electrode materials is close to the same. For the oxidation of

$\text{V}(\text{acac})_3$ , the peak separation change on all electrode materials is about  $20\text{ mV}$ , while the reduced  $\text{V}(\text{acac})_3$  peak separation change on the platinum electrode is up to  $70\text{ mV}$ . This indicates that the oxidation of  $\text{V}(\text{acac})_3$  is quasi-balanced while its reduction rate is slower. The redox kinetics of  $\text{V}(\text{acac})_3$  were studied by using LSV, and the two-step reaction mechanism was fitted. The electron transfer rate of the  $\text{V}(\text{acac})_3/\text{V}(\text{acac})_3^+$  redox reaction is very fast, and the exchange current density of  $\text{V}(\text{acac})_3^-/\text{V}(\text{acac})_3$  on glass carbon, platinum and gold is  $1.3$ ,  $3.8$  and  $8.4\text{ A m}^{-2}$ , respectively, with a similar order of magnitude, indicating a similar electron transfer mechanism on all three electrode materials. They finally confirmed that the electrode material did not affect the redox kinetics of  $\text{V}(\text{acac})_3/\text{V}(\text{acac})_3^+$ , and secondly that the improvement in the reaction rate using gold or platinum was very small and could be overcome by using a high-surface-area carbon electrode. In order to improve the reversibility and kinetics of the redox electric pair, Almheiri et al.,<sup>[110]</sup> by combining the fast kinetics of the single iron (III) acetylacetone redox couple on the cathode side with the fastest of the chromium (III) acetylacetone redox couple on the negative side, prepared iron–chromium (Fe–Cr) NARFB with open-circuit voltage (OCV) of  $1.2\text{ V}$ . More importantly, the redox reaction on the cathode and anode sides of Fe–Cr NARFB is well positioned and can be quickly charged at voltages higher than the OCV of  $1.8\text{ V}$ , which is not previously reported in most NARFBs. In addition, the team adopted a composite NafionSi membrane with  $0.1\text{ M}$   $\text{Fe}(\text{acac})_3$  and  $\text{Cr}(\text{acac})_3$  as the active substance and  $0.4\text{ M}$   $\text{TEABF}_4$  as the supporting electrolyte, and measured CE and EE values as high as 99% and 53%, respectively, in the flow pool. The membrane contributes to a stable VE, thus maintaining a good initial DC after 50 cycles. However, the general performance characteristics of the proposed Fe–Cr NARFB are hampered by high internal resistance. Therefore, further attempts to overcome these limitations require constant research and development.

The complexes formed by ligands and metal atoms or metal ions through coordination bonds are called MCCs. MCCs have been used as electroactive substances in ORFBs due to their excellent electrical conductivity and solubility in any state. Preliminary results have shown that there is still much room for potential improvement in energy density and cycle life, so the research and development of metal complexes is currently in a relatively rapid stage of development, and there are constantly new organic substances being discovered and applied to ORFBs.

## 6. Summary and Outlook

The world is currently facing problems with optimizing and upgrading energy structures. The proportion of clean energy is increasing year by year, but wind power and photovoltaic power generation are discontinuous and unstable, so there is a huge demand for large-scale energy storage batteries. For large-scale energy storage batteries, the abundance of materials and their environmental impact after use are important factors to be considered. The active materials used in ORFBs are

composed of elements with high abundances, such as C, H, O, N, etc. The materials come from a wide range of sources and are, therefore, very suitable for large-scale energy storage. The detailed discussion in this paper shows that the application of metal complexes in ORFBs has a very bright future.

The metal complexes maintain a high solubility throughout the battery cycle, which is of great help in improving the energy density of the battery. It is believed that with the continued research and development of researchers, metal complexes will make significant contributions to the development of ORFBs. The following are our prospects for the application of metal complexes in ORFBs:

1. Wider electrode potential: By grafting different groups on ferrocene groups, changing the synthesis route of complexes and other methods, increasing the redox potential and improving the solubility of metal complexes in solvents.
2. Optimization of battery structure: Adjust or optimize the internal structure of the battery, increase the effective transmission quality of the active substance between the electrodes, and improve the electrochemical performance of the active substance.
3. Efficiency improvement: Researchers should focus on optimizing the performance of metal complexes to improve further the efficiency of ORFBs composed of metal complexes.
4. Extended life: It is expected to extend the cycle life of the battery as much as possible under the condition of low volume loss, which can also reduce the operating cost of the battery.
5. Low toxicity and sustainability: The constituent elements of these metal complexes are mainly derived from C, H, O, N and other elements with high abundance in nature, and their low toxicity and convenient recycling can meet the current needs of the world's sustainable development.
6. Reduced cost: It is also feasible to reduce the operating cost of the batteries by optimizing the synthesis routes and using cheaper and more readily available materials to synthesize the target products. By optimizing the synthesis route, the target products can be synthesized using cheaper and more readily available materials, thus reducing the operating cost of the battery, which is also feasible.
7. Advanced screening methods: The use of artificial intelligence methods assisted by machine learning technology and high-throughput screening methods to accurately design and select potential organic redox materials is expected to make greater breakthroughs in molecular structure.
8. Develop electrolytes with superior performance: suitable electrolytes should be highly conductive, non-toxic and corrosion-resistant. Therefore, further development is needed to find the best match between the active materials and the electrolytes to achieve high-performance ORFBs.

In summary, ORFBs are currently in a relatively rapid development stage, and the research of metal complexes as active materials for ORFBs is in the ascendant, and the preliminary research results are exciting. It is believed that metal complexes will be used to develop the next generation of

energy storage devices due to their excellent solubility and electrical conductivity. From the current point of view, the use of metal complexes as active materials in redox flow batteries will be the most mature technology for RFBs commercialization, so we expect more researchers to invest in the optimization of the structure and performance of metal complexes. We look forward to making more breakthroughs in low-cost, high-energy density and long-cycle life ORFBs to achieve practical applications of large-scale energy storage.

### Conflict of Interests

The authors declare no conflict of interest.

**Keywords:** Metal coordination compounds · Flow batteries · Renewable energy · Redox active materials · Electrolyte

- [1] K. Amini, A. N. Shocron, M. E. Suss, M. J. Aziz, *ACS Energy Lett.* **2023**, *8*, 3526–3535.
- [2] S. Belongia, X. Wang, X. Zhang, *Adv. Funct. Mater.* **2023**, *34*, 2302077.
- [3] Z. Manzoor Bhat, M. Furquan, M. Aurang Zeb Gul Sial, U. Alam, A. Saeed Alzahrani, M. Qamar, *J. Energy Chem.* **2024**, *95*, 499–510.
- [4] A. S. Metlay, B. Chyi, Y. Yoon, R. J. Wycisk, P. N. Pintauro, T. E. Mallouk, *ACS Energy Lett.* **2022**, *7*, 908–913.
- [5] X. Wei, L. Cosimescu, W. Xu, J. Z. Hu, M. Vijayakumar, J. Feng, M. Y. Hu, X. Deng, J. Xiao, J. Liu, V. Sprenkle, W. Wang, *Adv. Energy Mater.* **2014**, *5*, 1400678.
- [6] Y. Ding, G. Yu, *Angew. Chem. Int. Ed.* **2017**, *56*, 8614–8616.
- [7] Z. Li, T. Jiang, M. Ali, C. Wu, W. Chen, *Energy Storage Mater.* **2022**, *50*, 105–138.
- [8] R. P. Shekurov, V. A. Miluykov, D. R. Islamov, D. B. Krivolapov, O. N. Kataeva, T. P. Gerasimova, S. A. Katsyuba, G. R. Nasibullina, V. V. Yanilkin, O. G. Sinyashin, *J. Organomet. Chem.* **2014**, *766*, 40–48.
- [9] X. Wei, W. Pan, W. Duan, A. Hollas, Z. Yang, B. Li, Z. Nie, J. Liu, D. Reed, W. Wang, V. Sprenkle, *ACS Energy Lett.* **2017**, *2*, 2187–2204.
- [10] E. W. Zhao, T. Liu, E. Jónsson, J. Lee, I. Temprano, R. B. Jethwa, A. Wang, H. Smith, J. Carretero-González, Q. Song, C. P. Grey, *Nature* **2020**, *579*, 224–228.
- [11] X. Fang, Z. Li, Y. Zhao, D. Yue, L. Zhang, X. Wei, *ACS Materials Lett.* **2022**, *4*, 277–306.
- [12] B. Li, J. Liu, *Natl. Sci. Rev.* **2017**, *4*, 91–105.
- [13] M. L. Perry, K. E. Rodby, F. R. Brushett, *ACS Energy Lett.* **2022**, *7*, 659–667.
- [14] Y. Jiang, Z. Liu, Y. Lv, A. Tang, L. Dai, L. Wang, Z. He, *Chem. Eng. J.* **2022**, *443*, 136341.
- [15] L. Xia, W. Huo, H. Zhang, K. Xu, Y. Qing, F. Chu, C. Zou, H. Liu, Z. a. Tan, *ACS Appl. Energ. Mater.* **2022**, *5*, 1984–1991.
- [16] Y. K. Zeng, T. S. Zhao, X. L. Zhou, L. Wei, H. R. Jiang, *J. Power Sources* **2016**, *330*, 55–60.
- [17] Z. Li, Y. C. Lu, *Adv. Mater.* **2020**, *32*, 363–368.
- [18] L. Xia, W. Huo, H. Gao, H. Zhang, F. Chu, H. Liu, Z. a. Tan, *J. Power Sources* **2021**, *498*, 229896.
- [19] J. Noack, N. Roznyatovskaya, J. Kunzendorf, M. Skyllas-Kazacos, C. Menictas, J. Tübke, *J. Energy Chem.* **2018**, *27*, 1341–1352.
- [20] M. Schnucklak, S. Kuecken, A. Fetyan, J. Schmidt, A. Thomas, C. Roth, *J. Mater. Chem. A* **2017**, *5*, 25193–25199.
- [21] G. Yang, Y. Zhu, Z. Hao, Q. Zhang, Y. Lu, Z. Yan, J. Chen, *Adv. Energy Mater.* **2024**, *14*, 2400022.
- [22] N. Poli, M. Schäffer, A. Trovò, J. Noack, M. Guarneri, P. Fischer, *Chem. Eng. J.* **2021**, *405*, 126583.
- [23] G. D. De La Garza, A. P. Kaur, I. A. Shkrob, L. A. Robertson, S. A. Odom, A. J. McNeil, *J. Mater. Chem. A* **2022**, *10*, 18745–18752.
- [24] H. R. Jiang, J. Sun, L. Wei, M. C. Wu, W. Shyy, T. S. Zhao, *Energy Storage Mater.* **2020**, *24*, 529–540.
- [25] Z. Na, X. Sun, L. Wang, *Carbon* **2018**, *138*, 363–368.
- [26] Y. Shi, Z. Wang, Y. Yao, W. Wang, Y.-C. Lu, *Energy Environ. Sci.* **2021**, *14*, 6329–6337.

- [27] X. Wei, G.-G. Xia, B. Kirby, E. Thomsen, B. Li, Z. Nie, G. G. Graff, J. Liu, V. Sprenkle, W. Wang, *J. Electrochem. Soc.* **2015**, *163*, A5150–A5153.
- [28] Y. Yao, Z. Wang, Z. Li, Y. C. Lu, *Adv. Mater.* **2021**, *33*, 2008095.
- [29] Y. Ding, C. Zhang, L. Zhang, Y. Zhou, G. Yu, *Chem* **2019**, *5*, 1964–1987.
- [30] J.-E. Jang, S. Jayasubramaniyan, S. W. Lee, H.-W. Lee, *ACS Energy Lett.* **2023**, *8*, 3702–3709.
- [31] J. Lei, Y. Yao, Y. Huang, Y.-C. Lu, *ACS Energy Lett.* **2022**, *8*, 429–435.
- [32] M. Pugach, V. Vyshinsky, A. Bischi, *Appl. Energy* **2019**, *253*, 113533.
- [33] M. Rychcik, M. J. J. o. P. S. Skyllas-Kazacos, *J. Power Sources* **1987**, *19*, 45–54.
- [34] P. Leung, A. A. Shah, L. Sanz, C. Flox, J. R. Morante, Q. Xu, M. R. Mohamed, C. Ponce de León, F. C. Walsh, *J. Power Sources* **2017**, *360*, 243–283.
- [35] D.-Y. Wang, R. Liu, W. Guo, G. Li, Y. Fu, *Coord. Chem. Rev.* **2021**, *429*, 213650.
- [36] G. Yang, Y. Zhu, Z. Hao, Y. Lu, Q. Zhao, K. Zhang, J. Chen, *Adv. Mater.* **2023**, *35*, 2301898.
- [37] J. J. Orgill, C. Chen, C. R. Schirmer, J. L. Anderson, R. S. Lewis, *Biochem. Eng. J.* **2015**, *94*, 15–21.
- [38] Z. Hu, Z. Miao, Z. Xu, X. Zhu, F. Zhong, M. Ding, J. Wang, X. Xie, C. Jia, J. Liu, *Chem. Eng. J.* **2022**, *450*, 138377.
- [39] W. Lee, G. Park, Y. Kim, D. Chang, Y. Kwon, *Chem. Eng. J.* **2020**, *398*, 125610.
- [40] Y. Shi, C. Eze, B. Xiong, W. He, H. Zhang, T. M. Lim, A. Ukil, J. Zhao, *Appl. Energy* **2019**, *238*, 202–224.
- [41] S. J. Yoon, S. Kim, D. K. Kim, S. So, Y. T. Hong, R. Hempelmann, *Carbon* **2020**, *166*, 131–137.
- [42] L. Xia, Y. Zhang, H. Zhang, S. Jiang, Q. Lv, W. Huo, F. Chu, F. Wang, H. Li, Z. a. Tan, *Sustain. Energy Fuels* **2022**, *6*, 2045–2052.
- [43] S. Qi, L. Dai, W. Huo, Y. Jiang, S. Yuan, Y. Xiao, Y. Liu, L. Wang, Z. He, *Composites Part B* **2023**, *265*, 153384.
- [44] M. Li, G. Agarwal, I. A. Shkrob, R. T. VanderLinden, J. Case, M. Prater, Z. Rhodes, R. S. Assary, S. D. Minteer, *J. Mater. Chem. A* **2021**, *9*, 23563–23573.
- [45] Y. Fu, A. Howard, C. Zeng, Y. Chen, P. Gao, P. Stinis, *ACS Energy Lett.* **2024**, *9*, 2767–2774.
- [46] D. G. Kwabi, Y. Ji, M. J. Aziz, *Chem. Rev.* **2020**, *120*, 6467–6489.
- [47] K. Peng, G. Tang, C. Zhang, X. Yang, P. Zuo, Z. Xiang, Z. Yao, Z. Yang, T. Xu, *J. Energy Chem.* **2024**, *96*, 89–109.
- [48] T. Yin, J. Duanmu, L. Liu, *J. Mater. Chem. A* **2024**, *12*, 15519–15540.
- [49] H. Li, H. Fan, B. Hu, L. Hu, G. Chang, J. Song, *Angew. Chem. Int. Ed.* **2021**, *60*, 26971–26977.
- [50] L. Cao, M. Skyllas-Kazacos, C. Menictas, J. Noack, *J. Energy Chem.* **2018**, *27*, 1269–1291.
- [51] A. M. Fenton, R. K. Jha, B. J. Neyhouse, A. P. Kaur, D. A. Dailey, S. A. Odom, F. R. Brushett, *J. Mater. Chem. A* **2022**, *10*, 17988–17999.
- [52] Z. Han, T. Wang, Y. Cai, S. Rong, J. Ma, L. Hou, Y. Ji, *Carbon* **2024**, *222*, 135644.
- [53] M. Shoaib, P. Vallayil, N. Jaiswal, P. Iyapazham Vaigunda Suba, S. Sankararaman, K. Ramanujam, V. Thangadurai, *Adv. Energy Mater.* **2024**, 134755.
- [54] Y. Ji, M. A. Goulet, D. A. Pollack, D. G. Kwabi, S. Jin, D. De Porcellinis, E. F. Kerr, R. G. Gordon, M. J. Aziz, *Adv. Energy Mater.* **2019**, *9*, 217–225.
- [55] A. M. Kossuttaarachchi, T. R. Cook, *Electrochim. Acta* **2018**, *261*, 296–306.
- [56] M. Wu, M. Bahari, E. M. Fell, R. G. Gordon, M. J. Aziz, *J. Mater. Chem. A* **2021**, *9*, 26709–26716.
- [57] Y. H. Wan, J. Sun, Q. P. Jian, X. Z. Fan, T. S. Zhao, *J. Mater. Chem. A* **2022**, *10*, 13021–13030.
- [58] Z. Liang, R. K. Jha, T. M. Suduwella, N. H. Attanayake, Y. Wang, W. Zhang, C. Cao, A. P. Kaur, J. Landon, S. A. Odom, *J. Mater. Chem. A* **2022**, *10*, 24685–24693.
- [59] H. Chen, G. Cong, Y.-C. Lu, *J. Energy Chem.* **2018**, *27*, 1304–1325.
- [60] K. Amini, E. F. Kerr, T. Y. George, A. M. Alfaraidi, Y. Jing, T. Tsukamoto, R. G. Gordon, M. J. Aziz, *Adv. Funct. Mater.* **2023**, *33*, 134772.
- [61] W. Li, J. Li, X. Yuan, Z. Xiang, Z. Liang, Z. Fu, *J. Mater. Chem. A* **2023**, *11*, 19308–19311.
- [62] R. W. Hogue, K. E. Toghill, *Curr. Opin. Electrochem.* **2019**, *18*, 37–45.
- [63] S. Giri, I. Dash, *J. Mater. Chem. A* **2023**, *11*, 16458–16493.
- [64] P. Baldaguez Medina, V. Ardila Contreras, F. Hartmann, D. Schmitt, A. Klimek, J. Elbert, M. Gallei, X. Su, *ACS Appl. Mater. Interfaces* **2023**, *15*, 22112–22122.
- [65] T. Ma, Z. Pan, L. Miao, C. Chen, M. Han, Z. Shang, J. Chen, *Angew. Chem. Int. Ed.* **2018**, *57*, 3158–3162.
- [66] R. Rubio-Presa, L. Lubián, M. Borlaf, E. Ventosa, R. Sanz, *ACS Materials Lett.* **2023**, *5*, 798–802.
- [67] D. Schmitt, S. M. Abdel-Hafez, M. Tummeley, V. Schünemann, M. Schneider, V. Presser, M. Gallei, *Macromolecules* **2023**, *56*, 7086–7101.
- [68] C. Wang, X. Li, B. Yu, Y. Wang, Z. Yang, H. Wang, H. Lin, J. Ma, G. Li, Z. Jin, *ACS Energy Lett.* **2020**, *5*, 411–417.
- [69] J. Winsberg, C. Stolze, S. Muench, F. Liedl, M. D. Hager, U. S. Schubert, *ACS Energy Lett.* **2016**, *1*, 976–980.
- [70] J. Friedl, M. A. Lebedeva, K. Porfyrikis, U. Stimming, T. W. Chamberlain, *J. Am. Chem. Soc.* **2018**, *140*, 401–405.
- [71] X. Deng, M. Hu, X. Wei, W. Wang, K. T. Mueller, Z. Chen, J. Z. Hu, *J. Power Sources* **2016**, *308*, 172–179.
- [72] L. Wang, M. Huang, K. Wan, Z. Fu, Z. Xiang, Z. Liang, *Adv. Funct. Mater.* **2023**, *34*, 153628.
- [73] J. Winsberg, T. Hagemann, T. Janoschka, M. D. Hager, U. S. Schubert, *Angew. Chem. Int. Ed.* **2016**, *56*, 686–711.
- [74] B. Hwang, M. S. Park, K. Kim, *ChemSusChem* **2014**, *8*, 310–314.
- [75] F. Pan, Q. Wang, *Molecules* **2015**, *20*, 20499–20517.
- [76] J. Yu, M. Salla, H. Zhang, Y. Ji, F. Zhang, M. Zhou, Q. Wang, *Energy Storage Mater.* **2020**, *29*, 216–222.
- [77] Y. Yao, H. Xu, Z. Tian, J. Zhang, F. Zhan, M. Yan, C. Jia, *ACS Appl. Energ. Mater.* **2021**, *4*, 8052–8058.
- [78] J. Montero, W. da Silva Freitas, B. Mecheri, M. Forchetta, P. Galloni, S. Licoccia, A. D'Epifanio, *ChemElectroChem* **2022**, *10*, 134662.
- [79] D. Fang, J. Zheng, X. Li, D. Wang, Y. Yang, Z. Liu, Z. Song, M. Jing, *Batteries* **2023**, *9*, 102264.
- [80] F. Zhu, W. Guo, Y. Fu, *Chem. Soc. Rev.* **2023**, *52*, 8410–8446.
- [81] J. Noack, N. Roznyatovskaya, T. Herr, P. Fischer, *Angew. Chem. Int. Ed.* **2015**, *54*, 9776–9809.
- [82] C. G. Armstrong, R. W. Hogue, K. E. Toghill, *J. Electroanal. Chem.* **2020**, *872*, 147762.
- [83] P. S. Borchers, M. Strumpf, C. Friebel, I. Nischang, M. D. Hager, J. Elbert, U. S. Schubert, *Adv. Energy Mater.* **2020**, *10*, 2001825.
- [84] P. S. Borchers, I. Anufriev, J. Vitz, H. Görls, J. Elbert, I. Nischang, M. D. Hager, U. S. Schubert, *Macromolecules* **2022**, *55*, 1576–1589.
- [85] S. Wan, H. Jiang, Z. Guo, C. He, X. Liang, N. Djilali, T. Zhao, *Energy Environ. Sci.* **2022**, *15*, 2874–2888.
- [86] Y. Yan, R. Walser-Kuntz, M. S. Sanford, *ACS Materials Lett.* **2022**, *4*, 733–739.
- [87] D. Xu, C. Zhang, Y. Zhen, Y. Li, *ACS Appl. Energ. Mater.* **2021**, *4*, 8045–8051.
- [88] B. R. Schrage, Z. Zhao, A. Boika, C. J. Ziegler, *J. Organomet. Chem.* **2019**, *897*, 23–31.
- [89] C. Zhang, L. Zhang, Y. Ding, S. Peng, X. Guo, Y. Zhao, G. He, G. Yu, *Energy Storage Mater.* **2018**, *15*, 324–350.
- [90] S. Kim, D. Kim, G. Hwang, J. Jeon, *J. Electroanal. Chem.* **2020**, *869*, 114131.
- [91] M. Mousavi, H. Dou, H. Fathiannasab, C. J. Silva, A. Yu, Z. Chen, *Chem. Eng. J.* **2021**, *412*, 128499.
- [92] B. Hu, C. DeBruler, Z. Rhodes, T. L. Liu, *J. Am. Chem. Soc.* **2017**, *139*, 1207–1214.
- [93] J. Luo, M. Hu, W. Wu, B. Yuan, T. L. Liu, *Energy Environ. Sci.* **2022**, *15*, 1315–1324.
- [94] H. Song, G. Kwon, C. Citek, S. Jeon, K. Kang, E. Lee, *ACS Appl. Mater. Interfaces* **2021**, *13*, 46558–46565.
- [95] B. Zhang, B. R. Schrage, A. Frkonja-Kuczin, S. Gaire, I. A. Popov, C. J. Ziegler, A. Boika, *Inorg. Chem.* **2022**, *61*, 8117–8120.
- [96] Y. Yao, J. Lei, Y. Shi, F. Ai, Y.-C. Lu, *Nat. Energy* **2021**, *6*, 582–588.
- [97] R.-X. Gao, Y.-Y. Gao, R.-J. Xie, L.-M. Han, *Chem. Pap.* **2019**, *74*, 895–901.
- [98] H. Chen, Z. Niu, J. Ye, C. Zhang, X. Zhang, Y. Zhao, *ACS Appl. Energ. Mater.* **2020**, *4*, 855–861.
- [99] X. Shen, N. Sinclair, J. Wainright, A. Imel, B. Barth, T. Zawodzinski, R. F. Savinell, *J. Electrochem. Soc.* **2021**, *168*, 060539.
- [100] E. S. Beh, D. De Porcellinis, R. L. Gracia, K. T. Xia, R. G. Gordon, M. J. Aziz, *ACS Energy Lett.* **2017**, *2*, 639–644.
- [101] P. J. Cabrera, X. Yang, J. A. Suttil, K. L. Hawthorne, R. E. M. Brooner, M. S. Sanford, L. T. Thompson, *J. Phys. Chem. C* **2015**, *119*, 15882–15889.
- [102] J. Mun, D.-J. Oh, M. S. Park, O. Kwon, H.-T. Kim, S. Jeong, Y. G. Kim, M.-J. J. o. T. E. S. Lee, *J. Electrochem. Soc.* **2018**, *165*, A215.
- [103] C. Yang, G. Nikiforidis, J. Y. Park, J. Choi, Y. Luo, L. Zhang, S. C. Wang, Y. T. Chan, J. Lim, Z. Hou, M. H. Baik, Y. Lee, H. R. Byon, *Adv. Energy Mater.* **2018**, *8*, 1702897.
- [104] C. G. Armstrong, K. E. Toghill, *J. Power Sources* **2017**, *349*, 121–129.

- [105] K. P. Smith, R. Rungta, A. A. Wang, C. W. Monroe, *J. Electrochem. Soc.* **2023**, *170*, 060510.
- [106] J. Conradie, E. Erasmus, *Results in Chemistry* **2023**, *5*, 100818.
- [107] Q. Liu, A. E. S. Sleightholme, A. A. Shinkle, Y. Li, L. T. Thompson, *Electrochem. Commun.* **2009**, *11*, 2312–2315.
- [108] Q. Liu, A. A. Shinkle, Y. Li, C. W. Monroe, L. T. Thompson, A. E. S. Sleightholme, *Electrochem. Commun.* **2010**, *12*, 1634–1637.
- [109] A. A. Shinkle, A. E. S. Sleightholme, L. T. Thompson, C. W. Monroe, *J. Appl. Electrochem.* **2011**, *41*, 1191–1199.
- [110] M. O. Bamgbopa, Y. Shao-Horn, S. Almheiri, *J. Mater. Chem. A* **2017**, *5*, 13457–13468.

---

Manuscript received: June 29, 2024  
Revised manuscript received: August 13, 2024  
Accepted manuscript online: August 17, 2024  
Version of record online: October 21, 2024

---